

## Microplastics from miscellaneous plastic wastes: Physico-chemical characterization and impact on fish and amphibian development

Patrizia Bonfanti<sup>a,1</sup>, Anita Colombo<sup>a,1</sup>, Melissa Saibene<sup>a</sup>, Giulia Motta<sup>a</sup>, Francesco Saliu<sup>a</sup>, Tiziano Catelani<sup>b</sup>, Dora Mehn<sup>c</sup>, Rita La Spina<sup>c</sup>, Jessica Ponti<sup>c</sup>, Claudia Cella<sup>c</sup>, Pamela Floris<sup>a</sup>, Paride Mantecca<sup>a,\*</sup>

<sup>a</sup> Department of Earth and Environmental Sciences, Research Centre POLARIS, University of Milano – Bicocca, Milano, Italy

<sup>b</sup> Interdepartmental Microscopy Platform, University of Milano – Bicocca, Milano, Italy

<sup>c</sup> European Commission, Joint Research Centre (JRC), Ispra, Italy

### ARTICLE INFO

Edited by: Professor Bing Yan

#### Keywords:

Microplastics  
Zebrafish  
*Xenopus laevis*  
Developmental toxicity  
Chorion  
Intestine

### ABSTRACT

Microplastic pollution represents a global problem with negative impacts on aquatic environment and organisms' health. To date, most of the laboratory toxicological studies on microplastics (MPs) have made use of single commercial micro and nano-polymers, which do not reflect the heterogeneity of environmental MPs. To improve the relevance of the hazard assessment, micrometer-sized plastic particles of miscellaneous non-reusable waste plastics, with size <100 µm and <50 µm (waste microplastics, wMPs), were characterized by microscopic and spectroscopic techniques and tested on developing zebrafish and *Xenopus laevis* by FET and FETAX assays respectively. Moreover, the modalities of wMP interaction with the embryonic structures, as well as the histological lesions, were explored by light and electron microscopy.

We have shown that wMPs had very heterogeneous shapes and sizes, were mainly composed of polyethylene and polypropylene and contained metal and organic impurities, as well as submicrometric particle fractions, features that resemble those of environmental occurring MPs. wMPs (0.1–100 mg/L) caused low rate of mortality and altered phenotypes in embryos, but established species-specific biointeractions. In zebrafish, wMPs by adhering to chorion were able to delay hatching in a size and concentration dependent manner. In *Xenopus* embryos, which open stomodeum earlier than zebrafish, wMPs were accumulated in intestinal tract, where produced mechanical stress and stimulated mucus overproduction, attesting an irritation response.

Although wMP biointeractions did not interfere with morphogenesis processes, further studies are needed to understand the underlying mechanisms and long-term impact of these, or even smaller, wMPs.

### 1. Introduction

Microplastics (MPs) have become an emerging concern worldwide for both human and environmental health due to their enormous intentional or unintended release to the environment, particularly in marine and freshwater aquatic systems, where they are accumulated (Auta et al., 2017; Li et al., 2020).

MPs (average particle size 1–5000 µm Ø, GESAMP, 2015) gather together a large variety of organic polymers and include both primary MPs produced for specific commercial purposes (e.g. microbeads in tooth paste or cosmetics, Cole et al., 2011; Fendall and Sewell, 2009) and secondary MPs derived by breakdown of any plastic good (Barnes

et al., 2009; Eriksen et al., 2014). It is estimated that primary MPs represent only a small part of the MPs present in the environment (Andrady, 2011; Rist and Hartmann, 2018). Most of them are instead represented by secondary MPs, whose spread rate is almost impossible to control due to indiscriminate disposal and inadequate waste management systems without proper recycling. Land based plastic sources end up into aquatic ecosystems and here, despite their recalcitrance, they are embrittled and fragmented by mechanical, chemical and biological processes, thus contributing to about 80% of plastic debris found in these environmental compartments (Andrady, 2017).

Secondary MPs usually result to have irregular in size, shape and composition, physico-chemical (P-chem) features that in different ways

\* Corresponding author.

E-mail address: [paride.mantecca@unimib.it](mailto:paride.mantecca@unimib.it) (P. Mantecca).

<sup>1</sup> These authors contributed equally to the work

may pose a risk to organisms (de Sá et al., 2018; Jabeen et al., 2018; Mazurais et al., 2015). In addition to the hazards arising from MPs direct toxicity and bioaccumulation, particularly if their size reaches the nanoscale, the health concerns may also derive from their ability to adsorb and convey other hydrophobic chemical pollutants, such as persistent organic pollutants and endocrine disruptors (Lee et al., 2014; O'Donovan et al., 2018; Rainieri et al., 2018; Wang et al., 2018). At the same time, plastic additives, such as alkyl-phenols, bisphenol and phthalates, can be leached out from MPs, adding further harmful chemicals to those absorbed from the environment (Barnes et al., 2009; Browne et al., 2013).

Several studies conducted under controlled laboratory conditions have recently reported that commercial polystyrene MPs possess the capability to accumulate into various aquatic organisms (Lu et al., 2016; Pitt et al., 2018). Field studies have evidenced that starting from the primary consumers, mainly represented by the zooplankton (Cole et al., 2013; Setälä et al., 2014), all the organisms composing the aquatic food web, from invertebrates to seabirds and fish (Alomar and Deudero, 2017; Cau et al., 2019; Giani et al., 2019; Sfriso et al., 2020) seem to be involved in the bioaccumulation process, including edible and commercial species (Bouwmeester et al., 2015; Browne et al., 2008; EFSA, 2016; Koongolla et al., 2020; Markic et al., 2019; Neves et al., 2015; Savoca et al., 2020).

In aquatic vertebrates, MPs accumulate especially within the digestive system, which is also the main primary target (Markic et al., 2019). Laboratory studies on larval and adult fish evidenced that, at the intestinal level, MPs can cause damages at the gut epithelium compromising the feeding activity and bringing to negative effects on growth parameters and survival (Jabeen et al., 2018; Lei et al., 2018; Naidoo and Glassom, 2019; Pannetier et al., 2020; Pedà et al., 2016). In addition, some studies on marine and freshwater fish species reported MP translocation from the gut to the circulatory system and consequent histological and metabolic injuries to other organs such as liver (Espinoza et al., 2019; Jabeen et al., 2018; Lu et al., 2016).

In the extensive literature regarding the impact of MPs on aquatic organisms, it is noteworthy the knowledge gap on their potential adverse effects on development, when embryos mainly undergo passive exposure to MPs during the delicate phase of morphogenesis and organ functional differentiation.

However, most of the studies on invertebrates and vertebrates, including embryonic stages, have investigated the uptake and distribution of commercial micro- and nanoplastics, mainly spherical and monodisperse polystyrene (PS) (De Felice et al., 2018; Duan et al., 2020; Messinetti et al., 2018; Pitt et al., 2018). Alternatively, other studies assessed the impact of leaching by comparing virgin versus beach-stranded pellets or artificially contaminated commercial MPs (Batel et al., 2018; Nobre et al., 2015). Despite having appropriate dimensions, the commercial MPs are overly simplified and do not reflect the modality of interaction with organisms of the heterogeneous environmental MPs (Phuong et al., 2016). Environmental secondary MPs, intended as mixtures of fragments of different shapes, composition and aggregation capacity are therefore worthy of additional research efforts.

To improve the knowledge on the possible effects of environmental MPs during the development of sensible target organisms, like fish and amphibians, in the present study we used the zebrafish (*Danio rerio*) and the African frog (*Xenopus laevis*) as ecologically-relevant experimental models. Recently, these animal models have been extensively used to study the biointeractions and toxicity of micro- and nano-particles (NPs) (Bonfanti et al., 2019, 2015; Colombo et al., 2017; Fiandra et al., 2020; Haque and Ward, 2018; Mantecca et al., 2015), confirming their capability to efficiently predict the hazard of environmental and biomedical particles. Moreover, the specific developmental strategies of fish and amphibians offer the opportunity to study how the interactions of MPs with different embryonic structures may affect the development.

In order to improve the relevance of the toxicological hazard assessment of the MP environmental pollution, micrometer-sized plastic

particles were produced by fragmentation of miscellaneous plastics derived from the collection of miscellaneous plastic wastes in municipal ecological platforms. After mechanical sieving of the particles, the two smallest fractions with size ranges 100–50 µm and less than 50 µm were retrieved. These samples have been considered representative of the environmentally occurring and measurable MPs, with a micron-scaled dimension conferring them the ability to effectively interact and be taken up by aquatic organisms. After a detailed P-chem characterization of the wMPs by microscopy (light, SEM, TEM) and spectroscopy (ATR-FTIR, Raman, TXRF) techniques, the toxic responses have been investigated by the Fish Embryo acute Toxicity (FET) test using zebrafish, and the Frog Embryo Teratogenesis Assay-*Xenopus* (FETAX); the modalities of the MP interaction with the biological structures, as well as the histological lesions, have been investigated by microscopy techniques.

## 2. Materials and methods

### 2.1. Production of waste plastic granules and microparticles

Plastic granulates were obtained from industrial partners in the framework of the project ECOPAVE (*POR FESR 2014–2020, Reg. Lombardia*), in which a pilot value chain has been established to collect and reuse plastic wastes. After being collected, the plastic waste of various origins was treated to obtain fractions of plastic granules of decreasing size (Text S2, [Supporting Information](#)) on which the ATR-FTIR analysis was carried out.

The finest wMP fractions, with at least one of the dimensions of 50 µm <wMPs <100 µm and wMPs <50 µm (named F1 and F2 respectively), have been used for further chemical-physical and toxicological analyses.

### 2.2. Waste microplastic characterization

#### 2.2.1. ATR-FTIR spectroscopy

Attenuated total reflection-Fourier-transform infrared (ATR-FTIR) spectroscopy analysis was performed using a Nicolet In5 FTIR instrument (Thermo Fisher Scientific) with 128 scans at 2 cm<sup>-1</sup> of resolution in the range of 4000–550 cm<sup>-1</sup>. Four sampling replicates were collected from each of the six different size fractions (Fig. S1 C). Applied contact force was increased until a constant ratio between the C-H stretching bands at 2900 cm<sup>-1</sup> and the CH<sub>2</sub> rocking bands at 720 cm<sup>-1</sup> was ensured. Spectral acquisition, analysis and library research were performed by using the OMNIC Spectra software. Identity confirmation was established with 95% match obtained with the patented comparison algorithm provided by the software.

#### 2.2.2. Raman spectroscopy

Raman spectroscopic analysis of the F1 and F2 wMP particles was performed using an alpha300 confocal Raman microscope (WITec, Ulm, Germany) applying a 532 nm laser. Particles were deposited using a stainless-steel spatula on a polished, clean silicon wafer placed on the motorized stage of the Raman microscope. For both fractions, spectra of 50 particles were collected using a 10x objective typically at 1 s integration times by averaging 10 accumulations. Materials were identified after baseline subtraction of the raw spectra, using the ACDLabs UVVis manager software and an in-house built polymer database. For the identification of materials not present in our database (polyethylene-octene copolymer) an open spectral database, OpenSpecy ([www.openspecy.org](http://www.openspecy.org)) (Cowger et al., 2021) was utilized. Spectra without specific Raman features (only wide fluorescent signal) were considered to be not-identified.

#### 2.2.3. Total reflection X-ray fluorescence (TXRF)

TXRF measurements were performed after sample digestion as previously described (Bobba et al., 2021) with some modification. Briefly wMP F1 and F2 samples (0.3 g) were placed in dried glass microwave

digestion tubes and dispersed in 800  $\mu\text{L}$  of aqua regia plus 100  $\mu\text{L}$  of 30%  $\text{H}_2\text{O}_2$  solution, added drop by drop. Three replicates for each wMP fraction were prepared. Samples were digested by an automatized CEM Explorer SPD microwave digestion system and treated at 220  $^\circ\text{C}$  for 10 min (after 10 min ramping to the final temperature). The digestion step was repeated twice by adding again the same amount of reagents in the same glass tube. Three blank samples were processed with the same digestion protocol operated with only aqua regia and  $\text{H}_2\text{O}_2$ . Samples and blanks were then purified using an Amicon Ultra-4 centrifugal filter, 100 kDa (Millipore), and diluted 1:1 in water. Mixture for TXRF analysis were prepared in triplicate by adding 10  $\mu\text{L}$  of each sample to 77  $\mu\text{L}$  of  $\text{HNO}_3$  at 14%w/v, 3  $\mu\text{L}$  Ga internal standard (3.3 mg/L final concentration), and 10  $\mu\text{L}$  Triton X-100 at 1.0% w/v. 5  $\mu\text{L}$  of the final mixture were spotted on acrylic sample holder, dried and placed in the TXRF spectrometer (S4 T-Star 4 TXRF spectrometer, Bruker) equipped with a Mo X-ray source. Measurement data were collected for 1200 s.

#### 2.2.4. Particle size and particle size distribution

The size and particle size distribution of F1 and F2 were determined by the laser diffraction method (Malvern Mastersizer 3000). The measurements were performed either in ethanol and 0.1% w/v Triton X-100 and kept under continuous stirring (850 rpm) during the analysis. Each measurement was performed in five replicates.

The model for data analysis assumes that the particle are not-spherical, while refractive index and absorption value were set to 1.5 and 0.010, respectively, on the base of the chemical composition of the material. Laser obscuration was kept between 10% and 20%. Data were reported as size distribution, calculated from the volume size distribution.

#### 2.2.5. Microscopy characterization

Light, Fluorescence, Scanning and Transmission Electron Microscopy (LM, FM, SEM and TEM-EDX) were used to characterize morphology, optical properties and elemental composition of F1 and F2. For LM analysis, small amounts of F1 and F2 granulates were mounted onto glass slides and observed under a Zeiss Axioplan microscope equipped with an Axiocam MRc5 digital camera. For FM, the slides were observed with an inverted Zeiss Observer.Z1 microscope, equipped with a Zeiss AxioCam MRm digital camera, selecting UV, eGFP and DsRed filters. For SEM analysis, F1 and F2 samples were attached with adhesive carbon tape onto stubs and sputter-coated with 10 nm gold. SEM-SE imaging was performed using a TESCAN Vega<sup>®</sup>XM 5136 SEM operating at 20 kV acceleration voltage. For TEM analysis, F1 and F2 fractions were directly embedded in epoxy resin and ultrafine slices were cut using Leica EM-UC7 ultramicrotome (Leica, Milan, Italy). Slices were analyzed by EDX in STEM mode using JEOL-JEM 2100 at 120 kV (JEOL, Italy) coupled with Bruker X-flash detector 5030 (Bruker Italy). The QUANTAX 200 software, in Hypermap mode, assessed elemental composition.

### 2.3. Embryotoxicity test

#### 2.3.1. Preparation of the wMP treatment suspensions

To obtain the suspensions for the embryos' treatment, F1 and F2 were suspended in FET (in mg/L  $\text{NaHCO}_3$  100, Instant ocean salt 100,  $\text{CaSO}_4$  190 for zebrafish) or FETAX (in mg/L  $\text{NaCl}$  625,  $\text{NaHCO}_3$  96,  $\text{KCl}$  30,  $\text{CaCl}_2$  15,  $\text{CaSO}_4 \cdot 2\text{H}_2\text{O}$  60, and  $\text{MgSO}_4$  70 for *X. laevis*) solution (pH 7.5–8.5) to achieve the maximum working concentration of 100 mg wMPs/L. These suspensions were vortexed to obtain a uniform distribution of particles and then sequentially diluted to generate the additional treatment concentrations (0.1, 1 and 10 mg/L). To date, MP amounts measured in the aquatic environment are extremely variable, therefore we have chosen a range comprising an environmental relevant concentration (0.1 mg/L) with reference to the contaminated areas (Naidoo and Glassom, 2019) up to concentrations likely representing hotspot pollution events (10 and 100 mg/L).

According to the guidelines of the FET (OECD TG 236, 2013) and

FETAX (ASTM, 1998), embryos of zebrafish and *Xenopus* control groups were incubated in standard FET and FETAX solution respectively and all the solutions/suspensions were changed daily.

#### 2.3.2. Fish embryo acute toxicity (FET)

Wild-type (AB strain) zebrafish were maintained as described in S3.

The acute toxicity of wMPs was determined as recommended by the OECD (OECD, 2013), with minor modifications. Within 3 h post-fertilization (hpf), groups of 20 embryos at same development stage, obtained by natural spawning of adult wild type AB zebrafish pairs ( $n = 6$ ), were randomly subdivided in four Petri dishes ( $\varnothing$  6.0 cm) containing 10 mL of FET solution (control group) or treatment suspension (F1 and F2 wMPs at 0.1–1–10–100 mg/L). Embryos were exposed in a thermostatic chamber at  $26 \pm 0.5$   $^\circ\text{C}$ , under static conditions. Lethal (coagulation, lack of somite formation, lack of detachment of the tail from the yolk sac, lack of the heartbeat) indicating acute toxicity and sublethal (e.g. oedemas, hatching rate and tail malformations) endpoints, were monitored at 24, 48, 72 and 96 hpf.

At the end of the exposure period, randomly selected embryos from each experimental group were anesthetized in 0.16 mg/mL MS-222 and 10 embryos were processed for histological analysis while the remaining were fixed with 10% neutral buffered formalin for head-tail length measurement with the digitizing software AxioVision (Zeiss, Germany).

#### 2.3.3. Frog embryo teratogenesis assay *Xenopus* - FETAX

*Xenopus* embryos were obtained by natural breeding of pairs ( $n = 3$ ) of adult *X. laevis* injected with HCG into the dorsal lymph sac (females: 300 IU; males: 150 IU) as previously described (Bonfanti et al., 2015). Embryotoxicity tests were conducted according to the standard guide for the FETAX (ASTM, 1998) performing three replicate definitive tests in the same experimental conditions, each conducted using embryos from a different male/female pair of *X. laevis*. Groups of 25 embryos at the midblastula stage (Stage 8), 5 hpf (Nieuwkoop and Faber, 1956) were randomly placed in Petri dishes ( $\varnothing$  6.0 cm) containing 10 mL of FETAX solution (control group) or treatment suspension. Two replicate dishes were used for each test concentration (F1 and F2 0.1–1–10–100 mg/L) while for control group four replicate dishes were used.

All Petri dishes were incubated in a thermostatic chamber at  $23 \pm 0.5$   $^\circ\text{C}$  and daily dead embryos were counted and removed. FETAX endpoints (i.e. mortality, malformations and growth inhibition) were considered at the end of the assay (stage 46, 96 hpf). At the end of the analysis, embryos ( $n = 75$  randomly selected from each experimental group) were fixed in 10% neutral buffered formalin to evaluate the growth retardation by measuring head-tail lengths with the digitizing software AxioVision (Zeiss, Germany). The remaining embryos were processed for the subsequent morphological analyses.

### 2.4. Fluorescence stereomicroscopy analysis of zebrafish and *Xenopus* embryos

The optical property of some wMPs emitting fluorescence has been exploited to localize the wMPs particles in order to evaluate their bio-interactions with embryonic tissues. To this aim, groups ( $n = 10$ ) of living zebrafish embryos at 24 hpf and formalin fixed *Xenopus* embryos at 96 hpf were randomly sampled from control and 100 mg/L F1 and F2 experimental groups and observed under a dissection microscope (Leica, M205FA equipped with LAS X Expert software) in brightfield and fluorescence mode with GFP long pass and DsRed filter settings.

### 2.5. Histological analyses

At the end of FET and FETAX (96 hpf), embryos ( $n = 10$ ) were randomly selected from control and 100 mg/L F1 and F2 experimental groups, fixed in Bouin's solution and processed for paraffin embedding. Samples were transversely cut from eye to proctodeum into 6  $\mu\text{m}$  thick serial sections, mounted on glass slides and stained with haematoxylin

and eosin (H&E) or Periodic acid–Schiff (PAS). The slides were screened under a Zeiss Axioplan optical microscope equipped with an Axiocam MRc5 digital camera.

## 2.6. Scanning electron microscopy of *Xenopus* embryos' intestines

For SEM analysis, 96 hpf embryos randomly selected at the end of the FETAX from the control, F1 and F2 wMPs 100 mg/L groups ( $n = 6$  each) were euthanized with MS-222 (300 mg/L). The intestinal tubes were dissected, immediately fixed overnight (ON) with 2% glutaraldehyde in Na-cacodylate (CAC) buffer (0.1 M), washed with CAC buffer (0.1 M) and post-fixed with 1% osmium tetroxide in CAC buffer (0.1 M) for 90 min at room temperature (RT). After dehydration with a graded ethanol series up to 100%, specimens were infiltrated with hexamethyldisilazane and left to dry ON at RT. After drying, the samples were placed on a conductive tape mounted on aluminum stubs and coated with 10 nm chromium using high vacuum Quorum Q150T-ES sputtering system. SEM-SE micrographs were acquired by means Zeiss Gemini 500 FEG-SEM operating with an acceleration voltage of 5 kV.

## 2.7. Data collection and statistical analysis

The number of dead embryos versus their total number at the beginning of the tests led to the mortality percentages and the number of malformed embryos versus the total number of surviving ones gave the

malformed embryo percentages. Data were expressed as the average  $\pm$  standard error (SE) or standard deviation (SD) and the percentage relative standard deviation (RSD %). Data were tested for homogeneity and normality and one-way analysis of variance (ANOVA) was performed. The daily and cumulative hatching percentages were investigated by chi-square method, using Yates's correction for continuity ( $\chi^2$  test) or Fisher's exact tests. The elaboration of cumulative hatching data of zebrafish embryos by probit analysis (Finney, 1971) allowed obtaining the median Hatching Time ( $HT_{50}$ ) value, which is the hatching time for 50% of the embryos. All statistical test were applied with at least 95% confidence interval using the IBM SPSS statistic 25 software.

## 3. Results

### 3.1. Microplastic characterization

The preliminary chemical characterization of the plastic granulates obtained from the collected plastic waste showed that poly-olefins were the main components (data not shown). After the dimension-based fractionation of the wMP granulate by manual sieving, additional chemical characterizations were performed to identify the type of polyolefin prevalent and any change in chemical structure induced by the grinding process in the different granule subpopulations. Representative ATR-FTIR spectra of these different sized fractions are presented in Fig. 1 A. The list of the main peaks detected is reported in

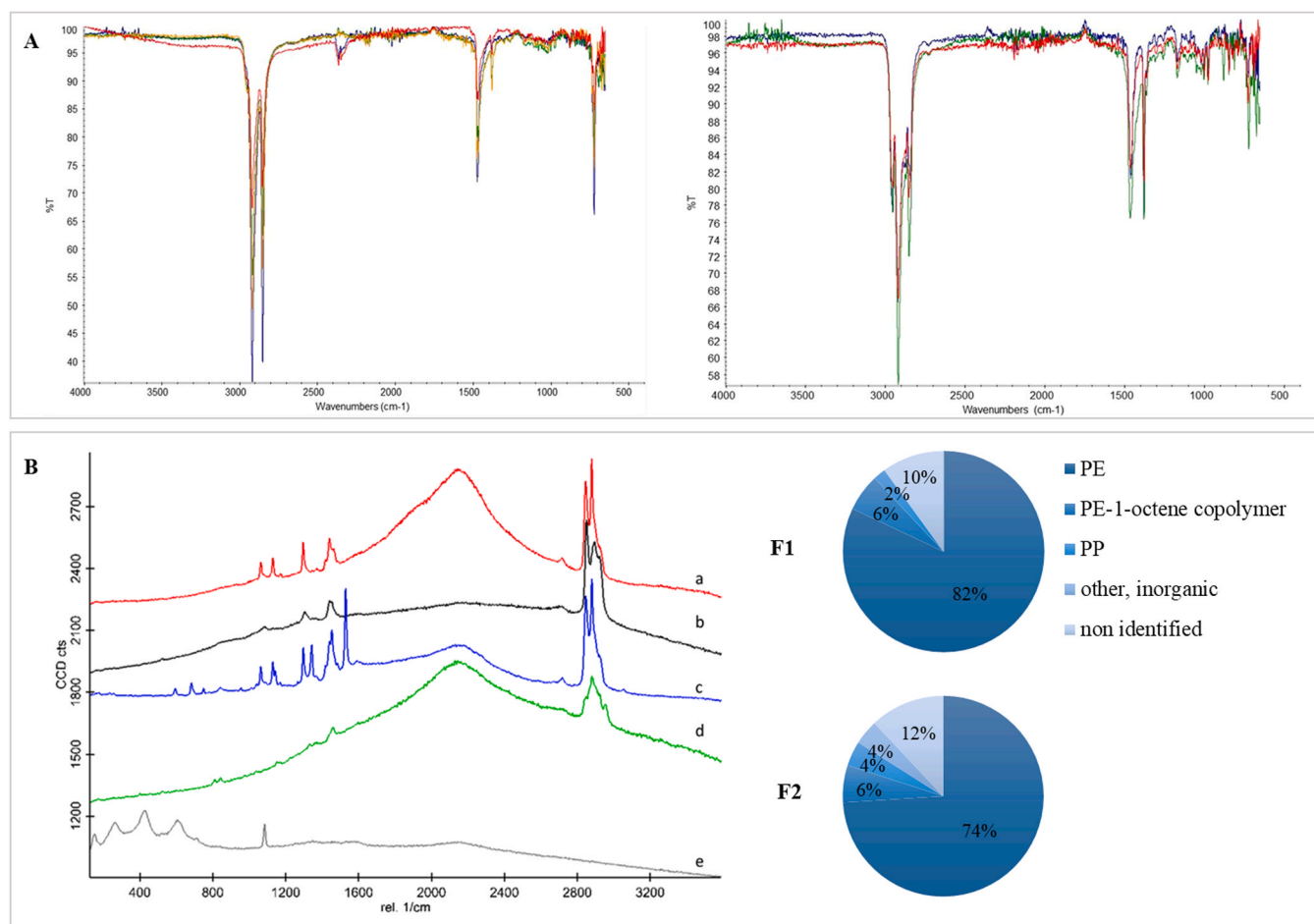


**Fig. 1.** Polymer characterization of wMPs. Panel A: superimposed ATR-FTIR spectra of polyethylene (left) and polypropylene (right) granulates obtained from each of the six dimensional fractions of wMPs. Panel B: Raman spectroscopy analysis of wMPs. On the right: examples of raw Raman spectra of the analyzed particles before baseline subtraction, many of them showing wide fluorescence peaks in addition to the Raman lines. From top to bottom: a) polyethylene, b) polyethylene-octene copolymer, c) polyethylene with phthalocyanine blue additive, d) polypropylene in fraction F1, e) metal oxide (rutile) containing particle in fraction F2. On the left: summary of the chemical composition of the wMP particles in fractions F1 and F2.

Table S1.

Considering a >85% match, library research enabled the identification of two main polymers: polyethylene (PE) and polypropylene (PP) in a 8:1 ratio. No other polymers were identified. Considering the same identified polymer in the different size fractions the spectra resulted similar, indicating that no remarkable transformation were induced in the chemical structure of the bulk material during the sorting and grinding process. However, some aliquots displayed peaks not detected in the reference virgin pellets, indicating that the original plastic materials were probably containing different ingredients that were retained during the processing and/or faced a different degradation pathway. Specifically, seven samples display signals at  $1719\text{ cm}^{-1}$  that may originate from oxidation processes of the aliphatic chain.

The finest fractions obtained in appreciable quantities from the sieving of initial granulate were F1 and F2 (Fig. S1 C), which comprise plastic particles with at least one nominal dimension between 100 and  $50\text{ }\mu\text{m}$  and less than  $50\text{ }\mu\text{m}$  respectively. These fractions were selected to study the impact on zebrafish and *Xenopus* embryonic development and their biointeraction potential. To support toxicological data, F1 and F2 wMPs were further characterized in terms of chemical compositions by Raman spectroscopy, TXRF and EDX, and of shape and dimension by laser diffraction and LM, FM, SEM and TEM analysis.

Characterization of F1 and F2 wMPs by Raman spectroscopy confirms the results obtained by FTIR on "bulk" aliquots, suggesting that most of the plastic particles are made of polyolefins (Fig. 1 B). Many of them also show fluorescence at the excitation wavelength applied, underlining that the waste plastic material contains several other ingredients beside the synthetic polymers. In the two fractions, about 74–82% of the particles were PE, 6% was PE copolymer, 2–4% were PP. Some of them contained also inorganic materials, like  $\text{TiO}_2$ . This is also confirmed by the TEM-EDX analysis, which shows the presence of different elements in nano-form such as Ti, Pb, Fe, Si, Al (Fig. 3 B). In

other cases, complex spectra revealed that many wMPs contained colorants like phthalocyanine blue (Simon and Röhrs, 2018). However, about 10–12% of the particles remained unidentified, in most cases because of the strong fluorescent signal of colorants/additives hiding the Raman features of polymers.

F1 and F2 fractions were also analysed by Total reflection X-ray fluorescence spectrometry (TXRF) to evaluate the presence of trace elements (Table S2). Overall, the F2 fraction shows higher concentration of extracted metals in comparison to F1. A more detailed analysis carried out by TEM-EDX shows the presence of Ti, Pb, Fe and Si in nanoform in the F1 fraction (Fig. 3 B, F1) whereas in the F2 fraction they were distributed more homogeneously inside the plastic particles (Fig. 3 B, F2).

The size and the volume size distribution of the two fractions were measured by the Mastersizer using ethanol and 0.1% Triton X-100 as dispersants (Table S3). The obtained values, which resulted higher than the nominal dimensions, might be affected by the presence of aggregates or agglomerates, as confirmed also by the variation of the volume size distribution observed in the different dispersant.

LM analysis confirmed the different size of the F1 and F2 wMP fractions and that particles are characterized by highly variable dimensions (even if within the limits imposed by the sieve), thickness, shapes and colours (Fig. 2 A). In addition to the round granules, also fibres and flakes with rough and sharp edges were observed. Moreover, since it is well known that plastic materials show significant autofluorescence when excited by near-UV or even visible radiation, F1 and F2 wMPs were observed with an inverted fluorescence microscope after selecting UV, GFP and DsRed filters (Fig. 2 B). Fluorescence images showed that the particles behaved differently in terms of fluorescence wavelength and intensity of emission. Considering that the fluorescence emission at a specific wavelength is intrinsic to the bulk polymer and can depend also on additives, pigments, impurities or degradation products

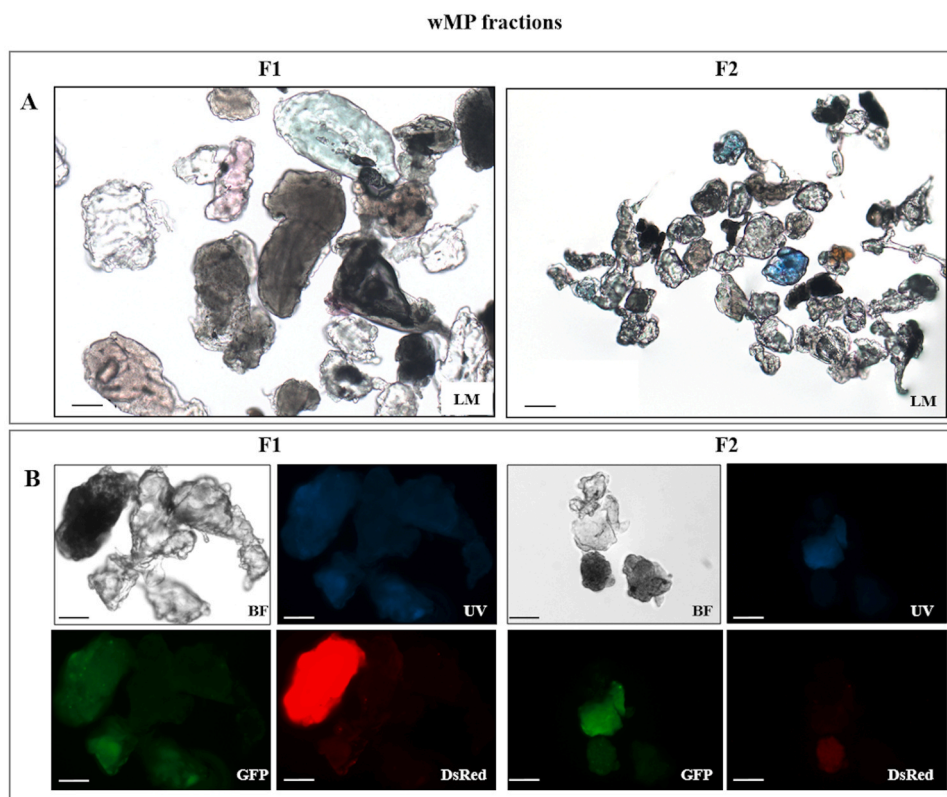


Fig. 2. Morphological characterization of wMPs. Representative light (A) and fluorescence microscope images (B) that highlight heterogeneity in terms of shapes, colors, sizes and optical properties of the particles contained in F1 and F2 fractions. LM=light microscope, BF=bright field. Filter setting for fluorescence microscope: UV= 358 nm, and GFP= 488 nm, DsRed= 563 nm. Scale bar =  $50\text{ }\mu\text{m}$ .

used in the production process (Hawkins and Yager, 2003; Qiu et al., 2015), this result confirms the presence of different polymers and various associated molecules in the selected fractions.

SEM analysis, performed to better characterize the wMP F1 and F2 morphology, confirmed that many particles have an irregular and rough surface and that submicrometric particles are aggregated to the surface of the larger ones (Fig. 3). TEM coupled with EDX confirmed the presence of nanoparticles inside F1 fraction slices and representative analysis showed Ti, Pb, Fe, Si alone or combined in nanoform of min Feret diameter around 100–200 nm (Fig. 3 B, F1). In the F2 fraction, elements such as Al, Pb, Fe and Si were more homogeneously distributed in the fraction, including also plastics particles of 1 µm size or less (Fig. 3 B, F2).

### 3.2. Effects of the wMPs on zebrafish and *Xenopus* embryos

A comparative evaluation of embryotoxicity of the F1 and F2 wMP fractions was conducted on zebrafish and *Xenopus laevis* during the first 96 h of development, a sensitive period that include important processes leading to organ formation.

FET results have evidenced that the exposure to both wMP fractions did not induce a significant increase in mortality and malformation rates in zebrafish embryos at 96 hpf (Fig. 4 A). The head-tail length of the embryos was also not substantially affected (Fig. S2). In contrast, a dose-dependent pattern was evidenced in the ability of zebrafish embryos exposed to both F1 and F2 wMPs to hatch successfully (Fig. 4 B). In particular, the evaluation of the daily hatching showed that the percentage of embryos exposed to F1 hatched mainly at 72 hpf with a dose-dependent decrease compared to unexposed ones. Instead, zebrafish embryos exposed to 0.1–10 mg/L F2 hatched at the same extent at 72 and 96 hpf, but those exposed to 100 mg/L hatched mainly at 96 hpf. The cumulative hatching rate highlighted the trend of embryos to delay the release from the chorion in a concentration-dependent manner, more marked for the finest fraction F2. However, at 96 hpf almost 100% of treated embryos were able to hatch similarly to controls. HT<sub>50</sub> values calculated at the different wMP concentrations confirmed that the time taken for hatching of 50% embryos was significantly delayed starting from 10 mg/L for F1 (HT<sub>50</sub> = 68.99 hpf) and from 1 mg/L for F2 (HT<sub>50</sub> = 74.30 hpf) respect to the control (HT<sub>50</sub> = 65.89 hpf) (Table S4).

We exploited the fluorescence of some plastic particles to highlight their adhesion to the chorion of 24 hpf zebrafish embryos as this interaction could be one of the causes influencing hatching (Fig. 4 B).

In control embryos, chorion surface appeared smooth and transparent unlike treated embryos, where some wMP aggregates attached to the chorion surface were observed as fluorescent spots. This result was more pronounced in F2 treated embryos. No fluorescent wMPs were detected in the periovular fluid and not even in the yolk sac or in other embryo tissues.

As with zebrafish, wMPs did not elicit mortality in *Xenopus* embryos since mortality rates for both fractions were not significantly different from control (Fig. 5 A). Malformation rates statistically different from controls (but never exceeding 10%) occurred sporadically, in particular to embryos exposed to F1 and F2 at 10 and 0.1 mg/L respectively, without any correlation with wMP concentration (Fig. 5 A).

However, the score of single malformations showed that the slight increase in malformation rates in treated embryos was mainly attributable to the loosening of the intestinal loops (Fig. 5 C). Observing embryos' abdominal region under dissecting microscope, the presence of debris in the loops of these slightly altered intestines was detected (Fig. 5 C). Taking advantage of the fluorescence emission properties of F1 and F2 fractions previously highlighted, the debris were identified to be mainly plastic particles (Fig. 5 C). It is likely that the presence of these wMP agglomerates in the gut lumen has interfered to a small extent with the tight coiling of the intestinal tube that characterizes *Xenopus* gut development. Furthermore, wMPs were only observed in the digestive tracts of F1 and F2 treated embryos while no particle was observed on

the epidermis or within other organs.

As far as it concerns the head-tail length of *Xenopus* embryos, a statistically significant increase respect to control was observed at all concentrations for the F1 and at 1 and 10 mg/L for F2 fractions (Fig. 5 B). Interestingly, a slight biphasic behaviour of the concentration-response curves of both fractions was observed, with the tendency of head-tail length to be greater at low or intermediate concentrations and lower at the high concentrations.

### 3.3. Bio-interactions of the wMPs with zebrafish and *Xenopus* embryonic tissues

In order to highlight the interactions of the wMPs with embryonic tissues and evaluate any damage induced to primitive organs, H&E transversal sections of control and 100 mg/L F1 and F2 exposed zebrafish and *Xenopus* embryos at 96 hpf were examined.

No histological and organ morphology alterations were detected in zebrafish embryos exposed to wMPs and no wMP fragments have been visualized inside the lumen or at the level of the yolk even in finest fraction (F2) treated embryos (Fig. S3). Furthermore, no altered phenotype of intestinal epithelium nor delay in intestinal development has been recorded in wMP treated embryos (Fig. 6, line D). Additional histological evidences regarding the distinct intestinal segments are reported in Fig. S3B.

In *Xenopus* embryos, although exposure to neither fractions of wMPs did result in morphological alterations of the primitive organs in the abdominal cavity (Fig. 6, line A) as in zebrafish, single heterogeneous fragments or agglomerates of wMPs were detected inside the lumen of several intestinal loops (Fig. 6, line B). In particular, the wMP particles seemed to adhere and press on the intestinal epithelium of these tracts, without causing apparent morphological damage to the epithelium.

Since mucus secreted by goblet cells provides a physical protection of intestinal epithelium and its hyper-production represents a physiological response to an undesirable irritant, a PAS staining was also performed. In the lumen of the intestinal loops of the control embryos, the reaction revealed a PAS positivity at the brush border level, consistent with the glycocalyx of microvilli membrane and the thin protective mucus layer stratified on the enterocytes (Fig. 6, line C). Instead, in the embryos exposed to both fractions of the wMPs, the reaction revealed a large amount of mucus into the lumen of some intestinal loops that wrap wMP particles (Fig. 6, line C). No presence of infiltrating inflammatory tissue was anyway observed at the level of the developing gut mucosa. At the level of the gill basket no wMP particle has been observed (Fig. S4).

SEM observation of isolated intestinal tube of *Xenopus* embryos exposed to 100 mg/L F1 and F2 has confirmed the accumulation of heterogeneous shaped and sized wMP particles in the digestive tract, which were so abundant to stuff the lumen (Fig. 7). The particles were found to be enclosed in a mucus coating and besides to pressing the microvilli of the enterocytes, some fibre-shaped and pointed fragments were wedged in the epithelium.

## 4. Discussion

MPs are recognized to pose a serious threat to various aquatic organisms, from detritus feeders to filter feeders and predators that, accidentally or intentionally, ingest them due to the similarities of these particles, so heterogeneous in size, shapes and colours, with their natural food sources (Botterell et al., 2019; Lusher, 2015).

The right concern that these plastic particles can accumulate in the digestive tract and starve wildlife triggered a rapid increasing number of studies especially focusing on the hazard deriving from the oral exposure route (Carbery et al., 2018).

Although these investigations still require attention to elucidate the modality of interaction of MPs with gut and the resulting mechanical and metabolic damage as well as the transfer of smaller particles to other

wMP fractions

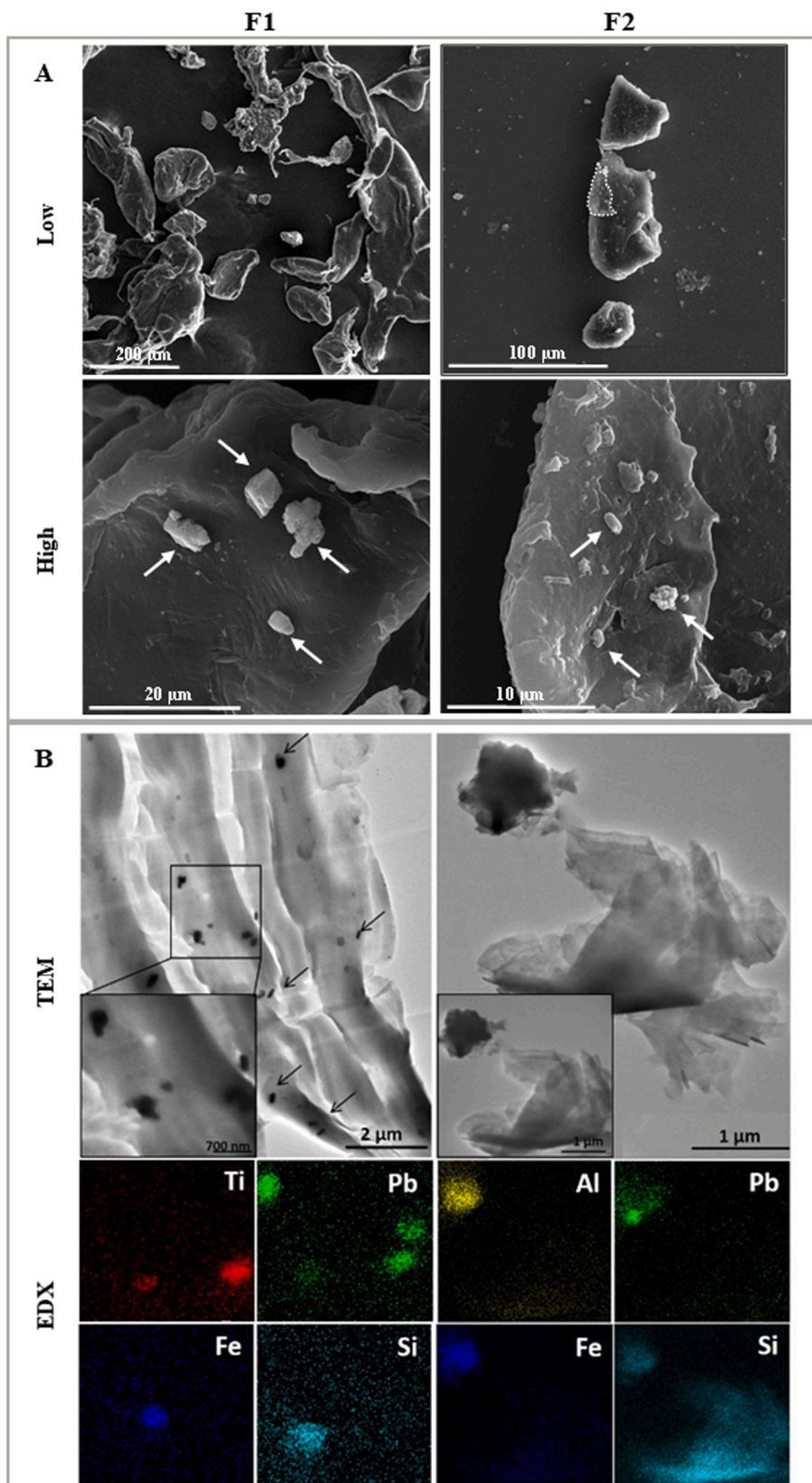


**Fig. 3.** Electron Microscopy analysis of wMPs. Panel A: SEM representative images at low and high magnification of F1 and F2 particles. It is possible to observe heterogeneous shapes and dimensions and the irregular surface of wMPs with the presence of sub-micrometric particles deposited on them (arrows). The high magnification of F2 corresponds to the white dotted area in low magnification image. Panel B: TEM images of F1 and F2 fractions ultrafine slices and corresponding EDX analysis in STEM mode (square selection and elemental maps). F1 fraction shows the presence of nanoparticles inside material of min Feret diameter around 100–200 nm (arrows) and the F2 fraction shows particles of min Feret diameter of 1 μm or less. The elemental composition of both fractions confirm the presence of Ti, Pb, Fe and Si in nano-form (F1 fraction) or distributed in the material (Al, Pb, Fe and Si in F2 fraction).

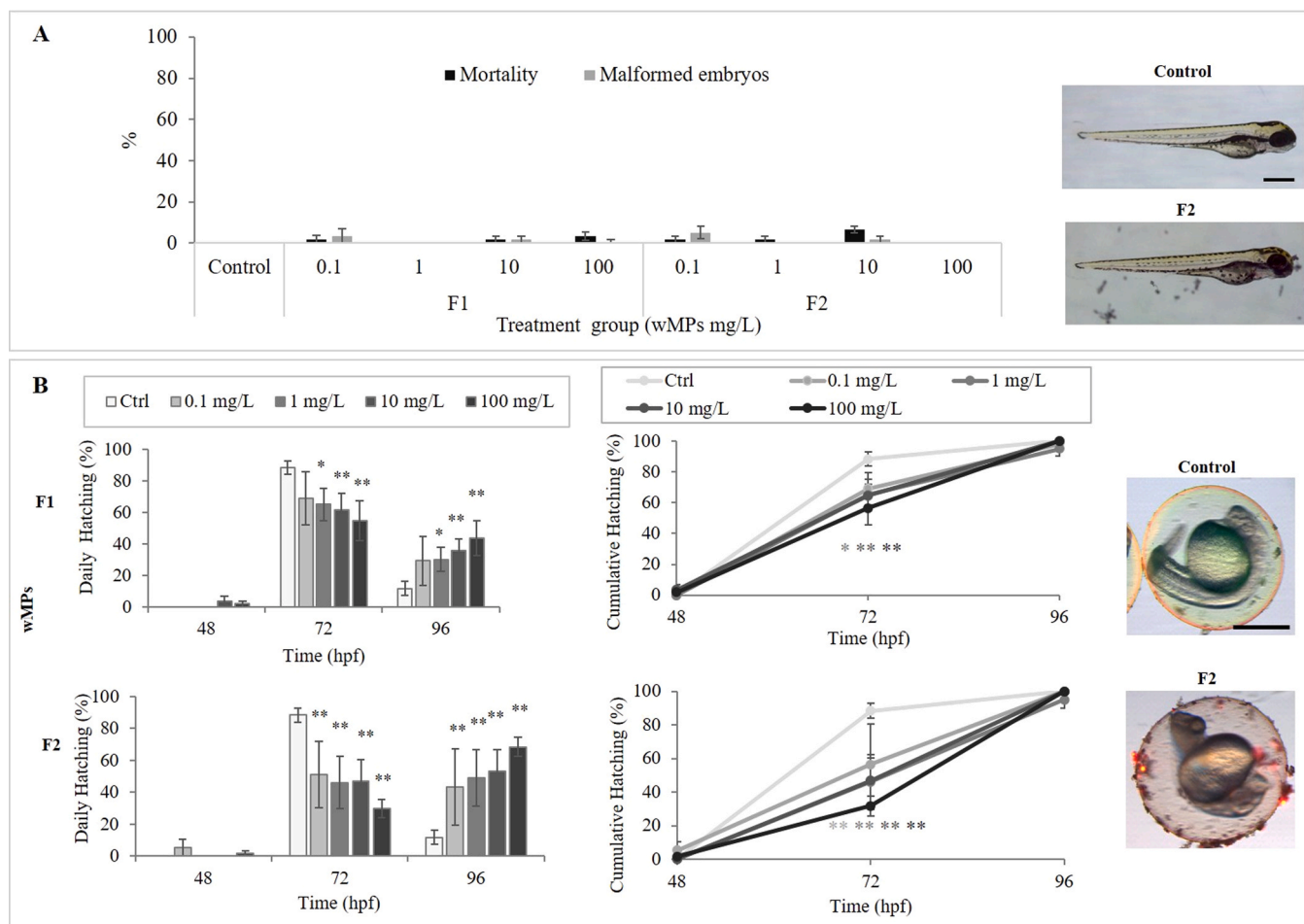


**Fig. 4.** Embryotoxicity of wMPs evaluated by FET. Panel A: mortality and malformation rates in 96 hpf embryos after exposure to F1 and F2 fractions (0.1–100 mg/L). On the right, representative stereomicroscopy images of a control embryo and a F2 exposed embryo at the end of assay (96 hpf). Panel B: daily and cumulative percentage of hatched control and wMPs exposed zebrafish embryos during FET. On the right, fluorescence stereomicroscopy representative images of control and F2 exposed zebrafish embryos at 24 hpf obtained by merging the red and green channels with bright field photographs. In wMP treated embryos, chorion surface is less smooth and transparent than in control and fluorescent wMP spots are observable. All values in the graphs are given as mean  $\pm$  SE of three independent assays. \*  $p < 0.05$ , \*\*  $p < 0.01$  indicate statistical difference from control (Chi-squared test). Scale bars = 500  $\mu$ m.

organs, it is important to advance knowledge on MP impact on embryonic life stage, before exogenous feeding, when the delicate phase of organogenesis is taking place. Moreover, on those aspects, almost none studies evaluated the impact of environmental secondary MPs deriving from wastes.

Thus, considering that of all the plastic produced less than 10% is recycled and the rest, if not destined for waste-to-energy, ends up into the environment (Alimi et al., 2018; Geyer et al., 2017), in this study we involved the finest MPs (100–50  $\mu$ m and < 50  $\mu$ m) retrievable by the mechanical fragmentation and sieving of non-reusable miscellaneous plastic waste. After a detailed P-chem characterization of the wMPs, we reported their effects on early development of two model organisms, *D. rerio* and *X. laevis*, widely exploited for (eco)toxicological studies on freshwater vertebrates under laboratory conditions.

The wMPs appear to share similarities with environmental MPs as referred to their chemical nature and morphology, without substantial differences between the two dimensional fractions considered. First of all, as suggested by Eitzen et al. (2019), the environmental relevance of the plastic materials tested should be one of the requirements for toxicological studies. According to FTIR and Raman analyses, our wMPs are mainly composed of PE and PP, a mixture of polymers highly representative of environmental MPs (Law, 2017).

The prevalence of these polymers was evidenced also in fragmented plastic samples collected on the beaches of known plastic accumulation

areas such as the North Atlantic (El Hadri et al., 2020) and North and South Pacific Ocean gyres (Pannetier et al., 2020). In addition, according to the origin of the starting plastic materials, some of the analysed wMP specimens showed a certain level of degradation such as oxidation, an aging process typical of environmental MP samples caused by atmospheric agents (Chen et al., 2019; Song et al., 2017). In this regard, testing in the laboratory a mixture of MPs composed of the most abundant polymers in the environment rather than a single commercial polymer, represents an innovative aspect of this study, which adds to the other environmentally relevant properties highlighted by the morphological characterization. Indeed, the heterogeneous shapes, the irregular surface texture and the highly variable particle size of our wMPs, are morphometric characteristics comparable to those of MPs sampled in the environment or extracted from the intestine of oceanic fish (Pannetier et al., 2020; Wang et al., 2017). Similar polymorphic MPs have also been reported by studies focusing on the standardization of procedures for the preparation of realistic MP suspensions, which are strongly recommended to improve the representativeness of aquatic MP laboratory research (Eitzen et al., 2019; El Hadri et al., 2020; Gigault et al., 2016). Another noteworthy result related to the surface of our wMPs is the presence of smaller particles with sub-micrometric dimensions attached to larger fragments, which leads us to hypothesize that this aggregation is due to wMP electrostatic and hydrophobic interactions, property that can be exploited to separate MPs from



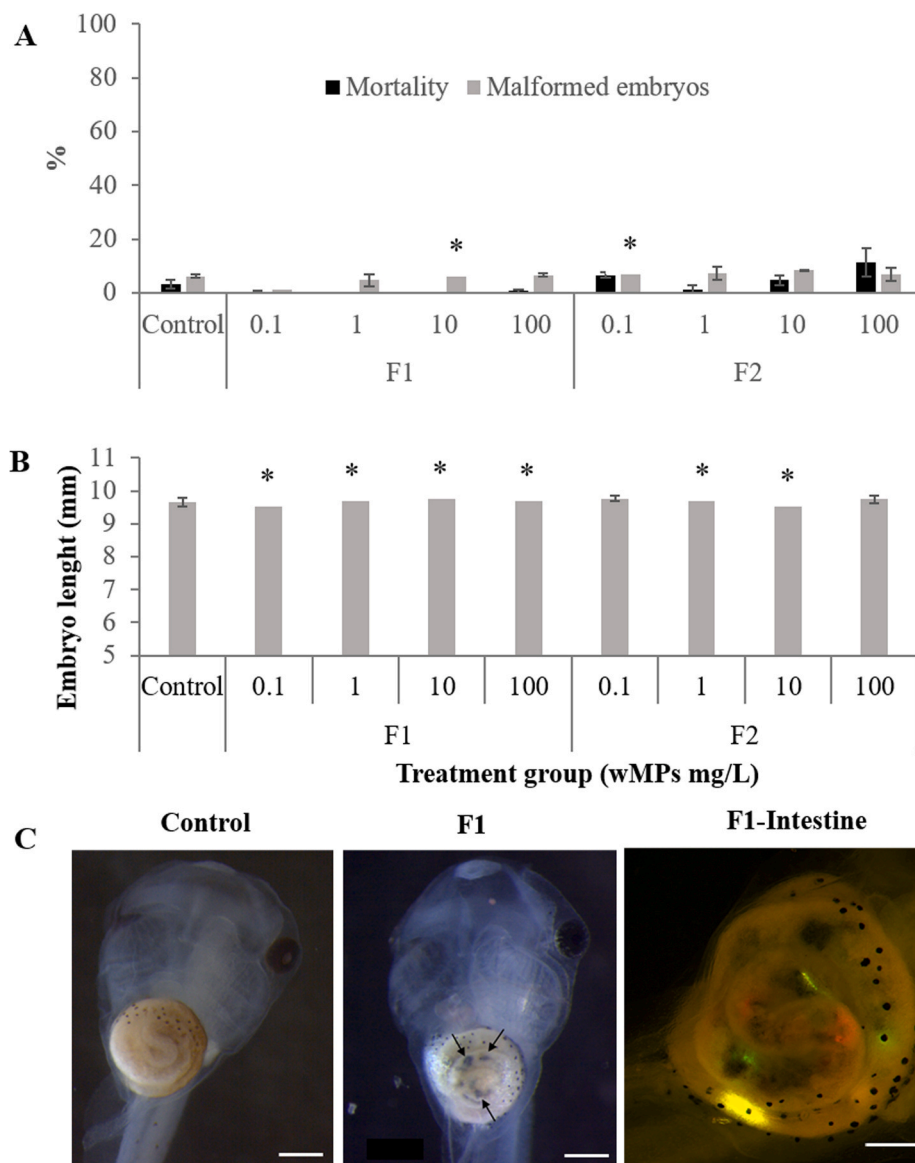


**Fig. 5.** Embryotoxicity of wMPs evaluated by FETAX. Mortality and malformation rates (A) and head-tail length (B) in 96 hpf embryos after exposure to F1 and F2 fractions (0.1–100 mg/L). All values are given as mean  $\pm$  SE of three independent assays. (\*) statistically different from control ( $p < 0.05$ , ANOVA + Fisher LSD Method). Panel C shows representative stereomicroscopic images of control and 100 mg/L F1 exposed embryos at the end of FETAX (stage 46–96 hpf), showing debris in the intestinal loops (arrows) of the latter. In the magnification of intestine of the 100 mg/L F1 exposed embryo observed at fluorescence stereomicroscopy (merge of the green and red fluorescence channels with the bright field photographs), it was ascertained that the most of the debris is represented by fragments of wMPs that emit fluorescence when excited in the GFP (green) or DsRed (red) channels. Scale bars = 500  $\mu$ m.

environmental samples (Felsing et al., 2018). This wide heterogeneity is highly representative of an environmental exposure, where MPs undergo to progressive size reduction, resulting in defragmentation into nanoplastics with diameter  $< 1 \mu$ m. These nanoscale plastic particles could be a significantly hazardous component even if hardly detectable in the environment (El Hadri et al., 2020; Ter Halle et al., 2017). In our case, the TEM-EDX analysis of F1 showed the presence of Ti, Pb, Fe, Si alone or combined in nanoform of min Feret diameter around 100–200 nm (Fig. 3 B, F1). In F2, elements such as Al, Pb, Fe and Si were mainly distributed inside the plastic particles. These particles a few  $\mu$ m in size or in the nanoscale could be even more harmful for organisms due to the greater ease of translocation through biological barriers and distribution with the circulatory system to the different tissues as demonstrated in mussels and zebrafish exposed to PS nanospheres (Browne et al., 2008; Lu et al., 2016; Pitt et al., 2018). Taking into consideration that our different polymeric wMPs also contain additives, impurities or degradation products used in the production process of the initial plastic materials, we verified that they show fluorescence emission at different wavelengths. This rarely used visualization strategy can be useful for detecting and isolating MPs from environmental samples (Fu et al., 2020; Savoca et al., 2020) but has also been proven well suitable for tracking wMPs in whole zebrafish and *Xenopus* embryos.

Based on FET and FETAX results, neither lethality nor phenotypic alterations were observed in neither zebrafish nor *Xenopus* embryos even at the highest F1 and F2 concentration tested. These results are in line with those obtained in zebrafish and *Xenopus* embryos exposed to commercial nano e microplastics that despite being distributed from the yolk sac to different organs or ingested did not affect survival and development (Batel et al., 2018; De Felice et al., 2018; Pitt et al., 2018). However, zebrafish embryo treatment with high PS nanoplastic concentrations via injection or waterborne exposure resulted in growth inhibition, increased frequency of malformations, hypoactivity and changes in neural and ocular genes expression (Zhang et al., 2020). Moreover, an anomalous embryonic development in two species of sea urchin and a slowdown of ascidian juveniles' metamorphosis were observed after external exposure to virgin PE pellets or after ingestion of PS beads (Messinetti et al., 2018; Nobre et al., 2015).

As regards the length of *Xenopus* embryos, recognized as one of the most sensitive indicator of developmental toxicity (ASTM, 1998), wMPs have led to a faint biphasic response related to the concentrations. This glimpses a possible hormetic effect that has been previously observed in developing amphibian exposed to other environmental stressors such as pesticides or metal oxide nanoparticles (Bolis et al., 2020). In particular, the stimulation of growth could be explained as an adaptive stress

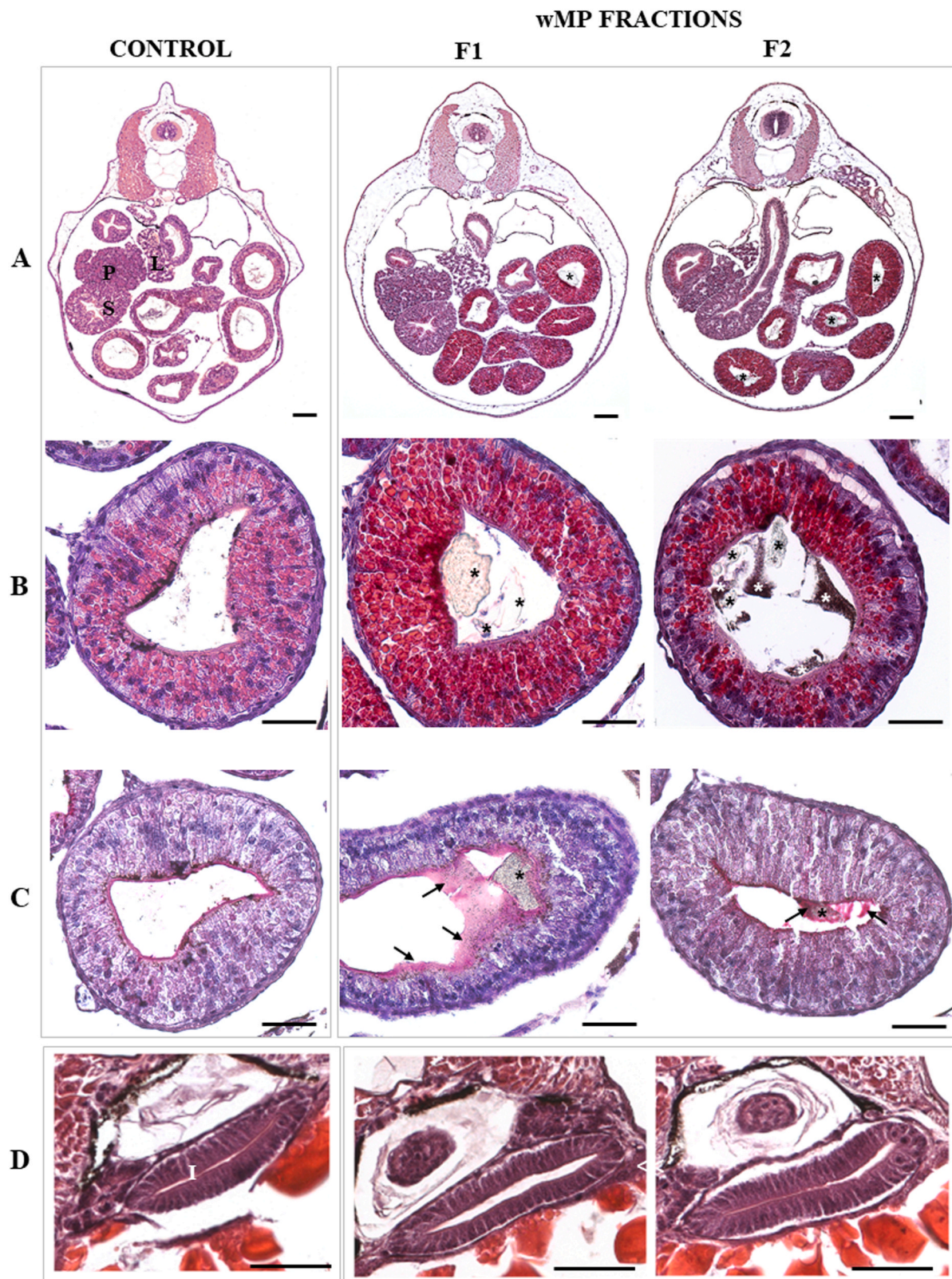


**Fig. 6.** Histological transversal sections of 96 hpf *Xenopus laevis* and zebrafish embryos at 96 hpf. Low magnification representative images H&E stained of whole *X. laevis* embryos showing that the localization and morphology of primitive organs in the abdominal cavity such as liver (L), pancreas (P), oesophagus-stomach transition (S) and intestine are not altered in wMP treated embryos compared to control. B) Magnification of an intestinal loop of a *Xenopus* embryo showing that several wMP particles (\*) are visible into the lumen, mainly attached to the surface of the lining epithelium, where they appeared to result in mechanical damage. C) PAS stained sections evidencing that mucus (arrows) is abundant and wrap wMPs in the F1 and F2 treated embryos. D) Magnifications of representative images of zebrafish embryos middle segment of intestine. No wMPs are detectable in intestinal lumen and intestinal epithelium is not altered in wMP treated embryos compared to control. (A-C) Scale bars = 100  $\mu$ m. (D) Scale bars = 50  $\mu$ m.

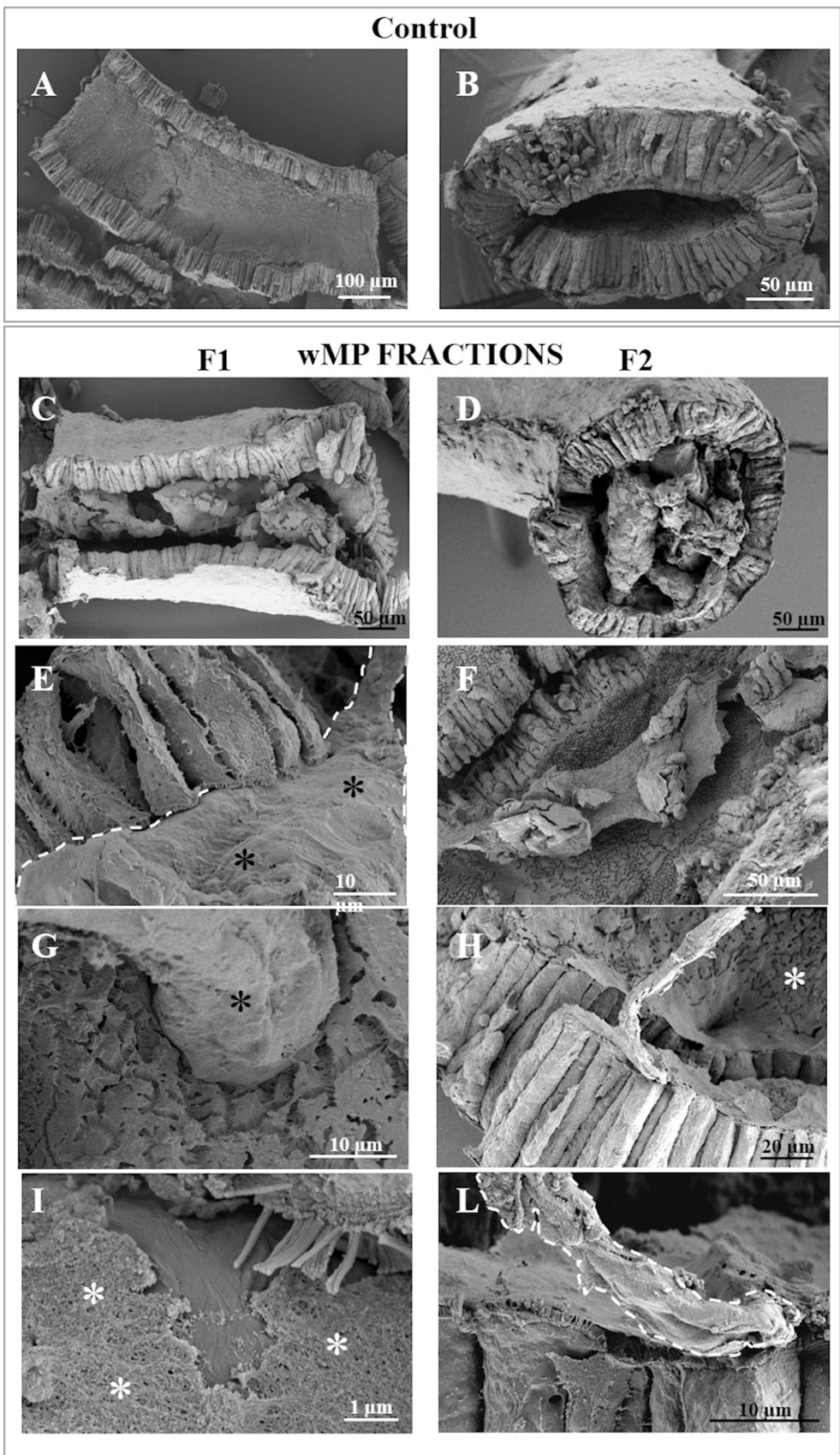


**Fig. 7.** SEM analysis of intestinal tube isolated from control and F1 and F2 wMP exposed *Xenopus* embryos. Representative images of intestinal epithelium from a control *Xenopus* embryo intestine (A, B) where the columnar morphology of enterocytes and the characteristic brush border facing to the lumen can be appreciated. In the representative images of the intestine isolate from embryos exposed to F1 (C, E, G, I) and F2 (D, F, H, L), the wMP fragments are crammed into the intestinal lumen and contact the microvilli, causing mechanical damage and hypersecretion of mucus that envelops them (white and black asterisks). In G the detail of a fibrous wMPs is visible that deepens in the epithelium. The dotted lines in E and L mark the wMP particles.

response to low, non-toxic concentrations of the environmental stressor.

Although not affecting the development of embryonic primary organs, morphological and histological analysis evidenced that wMPs interact with embryos' structures in species-specific manner due to the different morpho-functional peculiarities that characterize fish and amphibian development.

In particular, wMP treated zebrafish embryos displayed a temporary delayed hatching more marked in F2 fraction. By taking advantage of autofluorescence properties of some wMPs, we observed F2 much more than F1 particle aggregates attached to the chorion surface of 24 hpf zebrafish embryos. This analysis underestimates the amount of particles adhering to the chorion, as it does not highlight the non-fluorescent ones. Taking this into account, more particles may have adhered to the chorion, interfering with the mechanical tearing of the outermost thin layer caused by the tail movements of the embryo. Alternatively, the hatching delay could be attributed to a chemical action of the plastic additives, such as flame retardants as suggested by Lema et al. (2007) or of the metals present in both fractions. Reduced or delayed hatching has been reported after exposure to several metal oxide nanoparticles and attributed to the interaction of the nanoparticles with the zebrafish hatching enzymes (Ong et al., 2014). Batel et al. (2018) also observed that the 1–5  $\mu\text{m}$  MPs accumulated more on the outer surface of the zebrafish chorion than 10–20  $\mu\text{m}$  PE particles, but unfortunately did not report hatching data. Duan et al. (2020) found that PS particles have a high affinity for zebrafish chorions, causing a covering layer of PS particles on their outer surface. Since delayed hatching, more pronounced with nano PS, was observed, they hypothesized that PS could modify the mechanical properties of the chorions or affect the patency of their pores, leading to a hypoxic microenvironment in the embryos. It remains to establish if the wMPs effect on hatching is related to inhibition of hatching enzymes, change in mechanical properties of chorions or to environmental hypoxia and consequent impairment of embryo spontaneous movements.

No wMP fluorescent signals were instead observed in the periovular fluid. As expected, due to the pore size (500–700 nm), the chorion was found to be an effective barrier to all particles present in the two tested fractions, including those with sub-micrometric size. Similar results were reported in zebrafish embryos exposed to fluorescent PS particles ranging from 25 to 700 nm, which were excluded from the passage through chorion pores due to the surface charges or tendency to aggregation (van Pomeran et al., 2017). The barrier function of zebrafish chorions was also confirmed for nano PS in the diameter of 100 nm (Duan et al., 2020). Conversely, fluorescent PS and latex particles of about 50 nm used at low concentrations have proven to be able to penetrate zebrafish and medaka chorion respectively, initially accumulating in the yolk sac and later in other organs (Manabe et al., 2011; Pitt et al., 2018). These data suggest that the chorion represents a barrier capable of protecting the embryo in the crucial early stages of development from the impact with micrometric-sized MPs, while it does not exclude the passage of nanometric ones if present at low concentrations and not in aggregated form. Probably, the submicrometric particles present in our wMPs remained aggregated to the larger ones on the surface of the chorion or alternatively we were unable to map them with light microscopy inside the embryo.

Even in the post-hatching exposure interval up to 96 hpf, wMPs did not interact with the zebrafish embryonic tissues such as gills, epidermis or intestine via ingestion as confirmed both by microscopy observation. Similar results were obtained in zebrafish embryos treated with virgin and benzo [a] pyrene loaded MPs that after hatching remained mainly attached to the fish chorion, while not at all were found on the larval surface and only occasionally appeared within the gastrointestinal tract at 96 hpf (Batel et al., 2018). The absence of MP ingestion is consistent with the morpho-functional characteristics of the zebrafish embryo in the exposure window set by the FET protocol, in which the autonomous feeding is not yet active being the intestine not completely differentiated with the anus still closed and the yolk still available (Ng et al., 2005).

Consequently, uptake of the wMPs via the oral route cannot take place. Instead, by prolonging the exposure to 120 hpf, when the intestinal tract is a completely open-ended tube, the oral uptake of plastic particles becomes predominant as described by van Pomeran and colleagues (2017).

On the other hand, considering the amphibian *Xenopus*, the wMPs did not interfere with the hatching of embryo from the fertilization envelope that acts as a protective barrier up to stage 28 (32 hpf). Conversely, we found in a previous study that nanomaterials such as branched polyethyleneimine coated silver nanoparticles were able to modify fertilization envelope reducing and sometimes preventing *Xenopus* embryo hatching (Colombo et al., 2017). In the post hatching period, starting from stage 39–40 (56–66 hpf) when the stomodeum opens, *Xenopus* embryos acquire a characteristic swallowing and grazing behaviour facilitating intake of particles present in the surrounding environment (Bonfanti et al., 2019; Colombo et al., 2017). This behaviour caused a not selective assumption of wMPs via ingestion as occurs in aquatic filter feeding organisms such as copepods, cladocerans and ascidian juveniles (Cole et al., 2013; Messinetti et al., 2018; Rist et al., 2017).

The wMPs fluorescence optical properties facilitated the visualization of fluorescent spots in the intestinal lumen of whole embryos, discriminating them from any other debris physiologically present even in unexposed embryos. Histological and SEM analysis confirmed the presence of heterogeneous sized and shaped particles in the gut lumen and their interaction with the intestinal epithelium. wMPs, without any difference between F1 and F2 fractions, were visible close to or lying on the thin microvilli of enterocytes and sometimes entangled between them as evidenced by SEM images. This suggests a mechanical friction of wMPs on the apical surface of epithelium during intestinal transit depending on their irregular shapes, thus triggering an inflammatory response. It is well established that perturbed conditions such as infections or mechanical injury can induce mucin hypersecretion by goblet cells as a first defence strategy in mammals and fish (Cornick et al., 2015; Pedà et al., 2016). A gut responsiveness in terms of a hyper-secretion of mucus that trapped and enveloped wMPs in *Xenopus* embryos gut was observed. The property of mucus to entrap particles could avoid their contact with enterocytes' microvilli and protect the underlying tissues. Such a role had been highlighted in a previous study on *ex-vivo* pig ileum mucus blanket by implemented atomic force microscope, which proved to be able of binding and trapping particles up to 15  $\mu\text{m}$  in size (Sotres et al., 2017). The mucus trapping ability has been also observed towards plastic microfibers in other mucus secreting epithelia such as the skin of *Sardinia pilchardus* juveniles (Savoca et al., 2020). This finding shows how the mucus hypersecretion is an effective defence strategy already in developing *Xenopus* embryos, and confirms this model as a promising alternative to the use of adults in ingestion toxicology of environmental particles (Bonfanti et al., 2019).

To the best our knowledge, this is the first study that has investigated the interactions of environmentally relevant MPs from waste with *Xenopus* embryos' intestinal epithelium at histological level. In a previous study, De Felice and collaborators (2018) evidenced the ingestion of commercial 3  $\mu\text{m}$  PS beads by *Xenopus* embryos which, although clogging the lumen, did not cause any mechanical damage to the intestinal wall. Our results also confirm that wMPs induced slight damages to the intestinal epithelium, contrary to what we observed in *Xenopus* embryos exposed to more reactive metal-based nanoparticles (Bacchetta et al., 2012; Bonfanti et al., 2015; Colombo et al., 2017).

However, the mucus hypersecretion observed in this study highlights that the irregular shapes of the wMP fragments with sharp edges and rough surfaces and fibre-like structure can represent a physical risk for organism compared to those with spherical smooth shape, confirming the results of previous studies in adult fish (Jabeen et al., 2018). SEM images, where some wMPs appear even inserted into the epithelium, also support this idea.

Furthermore, no evidence that the two wMP fractions could invade

*Xenopus* embryos by routes other than the gastrointestinal tract were obtained. The same results were obtained also in zebrafish embryos exposed to PS MPs between 72 and 120 hpf, where the oral route was identified as the main one while skin exposure only marginally contributed to uptake and subsequent biodistribution (van Pomerren et al., 2017). In contrast, PS 70 nm nanoplastics, unlike PS 50  $\mu\text{m}$ , were able to penetrate muscle tissue through the epidermis of the goldfish *Carassius auratus* larvae, causing damage to muscle and nerve fibers (Yang et al., 2020).

For *Xenopus* embryos, the ingestion of environmentally relevant waste MPs does not interfere with growth as long as vitelline platelets are present in the enterocytes, but after 120 hpf the persistence of MPs knots in the gastrointestinal tract could cause obstruction leading to feeding impairment and death as described in *A. obstetricans* tadpoles feeding (from day 5) on periphyton contaminated with MPs (Boyero et al., 2020).

In addition, mucus hypersecretion could alter the physiological diffusion of ions and nutrients as well as the equilibrium of commensal bacteria, which in turn may contribute to chronic inflammatory diseases. For zebrafish embryos, the wMPs mainly impact by delaying hatching which may affect predatory escape behaviour and the later larval developmental stages, thus finally mining the fitness of the species.

## 5. Conclusion

In conclusion, wMPs obtained from miscellaneous plastic wastes and representative of environmental MP were characterized, confirming the highly heterogeneous size, morphology and composition, with PE and PP as main polymers. Submicrometric particles, as well the presence of metals and other organic co-contaminants are additional peculiarities of these MP samples. However, our results suggest that the effects of these complex materials are likely related to the shapes, texture surface and size of plastic particles rather than their chemical composition. Although wMPs did not severely interfere with early developmental processes and morphogenesis in zebrafish and *Xenopus*, they were able to establish specific biointeractions, depending on the peculiar structures and timing of the developmental patterning of the two species.

First, we demonstrated that wMPs are able to adhere to zebrafish chorion and delay hatching in a size and concentration dependent manner, without penetrating it, and confirming its role as an efficient physical barrier to micrometric plastic particles. Neither the epidermis nor the ingestion represented significant exposure route for zebrafish embryos to wMPs.

Instead, *Xenopus* embryos become more susceptible to wMPs exposure by ingestion during development. Due to swallowing behaviour, gastrointestinal tract was found to be the target organ of wMPs in this embryo model. The particle accumulation in the digestive diverticula likely produced a mechanical stress at the intestinal epithelium, resulting in blind morphological lesions and in an overproduction of mucus, which attests an irritation response of this tissue. These effects, occurring during development, may endanger the intestinal microenvironment, influence the organism's ability to feed and finally the possibility to correctly develop through larval and metamorphosis processes. Nevertheless, further experiments would be needed to evaluate changes in gene expression or metabolism to fully understand the toxicity of these wMPs.

In conclusion, the results of the present study strengthen the need of improving the knowledge on the biointeractions and mechanistic toxic effects of smaller MPs, including nanoplastics, from environmentally relevant waste plastic mixtures.

## Disclaimer

The scientific output expressed does not imply a policy position of the European Commission. Neither the European Commission nor any

person acting on behalf of the Commission is responsible for the use that might be made of this publication.

## Funding

This work was supported by ECOPAVE Project, Call Accordi per la Ricerca e l'Innovazione Cofin. POR FESR 2014–2020, Regione Lombardia.

## CRediT authorship contribution statement

**Patrizia Bonfanti:** Conceptualization, Methodology, Formal analysis, Writing – original draft, Writing – review & editing. **Anita Colombo:** Conceptualization, Methodology, Formal analysis, Writing – original draft, Writing – review & editing. **Melissa Saibene:** Investigation (FETAX test, LM, FM and SEM analysis), Formal analysis. **Giulia Motta:** Investigation (FET, FETAX test, LM and FM analysis). **Francesco Saliu:** Methodology, Investigation, Chemical analysis (ATR-FTIR). **Tiziano Catelani:** Methodology, Morphological analysis (SEM). **Dora Mehn:** Methodology, Investigation (Raman analysis). **Rita La Spina:** Methodology, Investigation (TXRF). **Jessica Ponti:** Methodology, Investigation (TEM-EDX analysis). **Claudia Cella:** Methodology, Investigation (Mastersizer analysis). **Pamela Floris:** Methodology, Investigation (FET, LM and FM analysis). **Paride Mantecca:** Conceptualization, Resources, Writing – review & editing, Supervision.

## Declaration of Competing Interest

The authors declare that they have no known competing financial interests or personal relationships that could have appeared to influence the work reported in this paper.

## Acknowledgements

This paper is dedicated to the memory of Prof. Marina Camatini, President of the Research Center POLARIS, University of Milano-Bicocca. Part of experimental data used in this research were generated through access to the Nanobiotechnology Laboratory under the Framework of access to the Joint Research Centre Physical Research Infrastructures of the European Commission (Wasteplastics project, Research Infrastructure Access Agreement Nr. RIAA\_35559). Authors thanks Pascal Colpo, Giacomo Ceccone, Francesco Fumagalli, European Commission, Joint Research Centre – Ispra. Authors wish also to thank the companies involved in the project ECOPAVE for the production of the waste plastic granules (Iterchimica srl, GEco srl) and the precious technical support of Mr. S. Cisani in this phase.

## Appendix A. Supporting information

Supplementary data associated with this article can be found in the online version at [doi:10.1016/j.ecoenv.2021.112775](https://doi.org/10.1016/j.ecoenv.2021.112775).

## References

- Alimi, O.S., Farner Budarz, J., Hernandez, L.M., Tufenkji, N., 2018. Microplastics and nanoplastics in aquatic environments: aggregation, deposition, and enhanced contaminant transport. *Environ. Sci. Technol.* 52, 1704–1724. <https://doi.org/10.1021/acs.est.7b05559>.
- Alomar, C., Deudero, S., 2017. Evidence of microplastic ingestion in the shark *Galeus melastomus Rafinesque, 1810* in the continental shelf off the western Mediterranean Sea. *Environ. Pollut.* 223, 223–229. <https://doi.org/10.1016/j.envpol.2017.01.015>.
- Andrady, A.L., 2011. Microplastics in the marine environment. *Mar. Pollut. Bull.* 62, 1596–1605. <https://doi.org/10.1016/j.marpolbul.2011.05.030>.
- Andrady, A.L., 2017. The plastic in microplastics: a review. *Mar. Pollut. Bull.* 119, 12–22. <https://doi.org/10.1016/j.marpolbul.2017.01.082>.
- ASTM, A.S. for T., 1998. Standard guide for conducting the frog embryo teratogenesis assay—*Xenopus* (FETAX). *Am. Soc. Test. Mater. Int.*
- Auta, H.S., Emenike, C.U., Fauziah, S.H., 2017. Distribution and importance of microplastics in the marine environment: a review of the sources, fate, effects, and

- potential solutions. *Environ. Int.* 102, 165–176. <https://doi.org/10.1016/j.envint.2017.02.013>.
- Bacchetta, R., Santo, N., Fascio, U., Moschini, E., Freddi, S., Chirico, G., Camatini, M., Mantecca, P., 2012. Nano-sized CuO, TiO<sub>2</sub> and ZnO affect *Xenopus laevis* development. *Nanotoxicology* 6, 381–398. <https://doi.org/10.3109/17435390.2011.579634>.
- Barnes, D.K.A., Galgani, F., Thompson, R.C., Barlaz, M., 2009. Accumulation and fragmentation of plastic debris in global environments. *Philos. Trans. R. Soc. B Biol. Sci.* 364, 1985–1998. <https://doi.org/10.1098/rstb.2008.0205>.
- Batel, A., Borchert, F., Reinwald, H., Erdinger, L., Braunbeck, T., 2018. Microplastic accumulation patterns and transfer of benzo[a]pyrene to adult zebrafish (*Danio rerio*) gills and zebrafish embryos. *Environ. Pollut.* 235, 918–930. <https://doi.org/10.1016/j.envpol.2018.01.028>.
- Bobba, S., Marques Dos Santos, F., Maury, T., Tecchio, P., Méhn, D., Weiland, F., Pekar, F., Mathieux, F., Ardenne, F., 2021. Sustainable use of Materials through automotive remanufacturing to boost resource efficiency in the road transport system (SMART). *Publ. Off. Eur. Union, Luxemb.* <https://doi.org/10.2760/84767>.
- Bolis, A., Gazzola, A., Pellitteri-Rosa, D., Colombo, A., Bonfanti, P., Bellati, A., 2020. Exposure during embryonic development to Roundup® Power 2.0 affects lateralization, level of activity and growth, but not defensive behaviour of marsh frog tadpoles. *Environ. Pollut.* 263, 114395. <https://doi.org/10.1016/j.envpol.2020.114395>.
- Bonfanti, P., Moschini, E., Saibene, M., Bacchetta, R., Rettighieri, L., Calabri, L., Colombo, A., Mantecca, P., 2015. Do nanoparticle physico-chemical properties and developmental exposure window influence nano ZnO embryotoxicity in *Xenopus laevis*? *Int. J. Environ. Res. Public Health* 12, 8828–8848. <https://doi.org/10.3390/ijerph120808828>.
- Bonfanti, P., Colombo, A., Saibene, M., Fiandra, L., Armenia, I., Gamberoni, F., Gornati, R., Bernardini, G., Mantecca, P., 2019. Iron nanoparticle bio-interactions evaluated in *Xenopus laevis* embryos, a model for studying the safety of ingested nanoparticles. *Nanotoxicology* 14, 196–213. <https://doi.org/10.1080/17435390.2019.1685695>.
- Botterell, Z.L.R., Beaumont, N., Dorrington, T., Steinke, M., Thompson, R.C., Lindeque, P. K., 2019. Bioavailability and effects of microplastics on marine zooplankton: a review. *Environ. Pollut.* 245, 98–110. <https://doi.org/10.1016/j.envpol.2018.10.065>.
- Bouwmeester, H., Hollman, P.C.H., Peters, R.J.B., 2015. Potential health impact of environmentally released micro- and nanoplastics in the human food production Chain: experiences from nanotoxicology. *Environ. Sci. Technol.* 49, 8932–8947. <https://doi.org/10.1021/acs.est.5b01090>.
- Boyero, L., López-Rojo, N., Bosch, J., Alonso, A., Correa-Araneda, F., Pérez, J., 2020. Microplastics impair amphibian survival, body condition and function. *Chemosphere* 244, 125500. <https://doi.org/10.1016/j.chemosphere.2019.125500>.
- Browne, M.A., Dissanayake, A., Galloway, T.S., Lowe, D.M., Thompson, R.C., 2008. Ingested microscopic plastic translocates to the circulatory system of the mussel, *Mytilus edulis* (L.). *Environ. Sci. Technol.* 42, 5026–5031. <https://doi.org/10.1021/es800249a>.
- Browne, M.A., Niven, S.J., Galloway, T.S., Rowland, S.J., Thompson, R.C., 2013. Microplastic moves pollutants and additives to worms, reducing functions linked to health and biodiversity. *Curr. Biol.* 23, 2388–2392. <https://doi.org/10.1016/j.cub.2013.10.012>.
- Carbery, M., O'connor, W., Thavamani, P., 2018. Trophic transfer of microplastics and mixed contaminants in the marine food web and implications for human health. *Environ. Int.* 115, 400–409. <https://doi.org/10.1016/j.envint.2018.03.007>.
- Cau, A., Avio, C.G., Dessì, C., Follesa, M.C., Moccia, D., Regoli, F., Pusceddu, A., 2019. Microplastics in the crustaceans *Nephrops norvegicus* and *Aristeus antennatus*: Flagship species for deep-sea environments? *Environ. Pollut.* 255, 113107. <https://doi.org/10.1016/j.envpol.2019.113107>.
- Chen, Q., Allgeier, A., Yin, D., Hollert, H., 2019. Leaching of endocrine disrupting chemicals from marine microplastics and mesoplastics under common life stress conditions. *Environ. Int.* 130, 104938. <https://doi.org/10.1016/j.envint.2019.104938>.
- Cole, M., Lindeque, P., Halsband, C., Galloway, T.S., 2011. Microplastics as contaminants in the marine environment: a review. *Mar. Pollut. Bull.* 62, 2588–2597. <https://doi.org/10.1016/j.marpolbul.2011.09.025>.
- Cole, M., Lindeque, P., Fileman, E., Halsband, C., Goodhead, R., Moger, J., Galloway, T. S., 2013. Microplastic ingestion by zooplankton. *Environ. Sci. Technol.* 47, 6646–6655. <https://doi.org/10.1021/es400663f>.
- Colombo, A., Saibene, M., Moschini, E., Bonfanti, P., Collini, M., Kasemets, K., Mantecca, P., 2017. Teratogenic hazard of BPEI-coated silver nanoparticles to *Xenopus laevis*. *Nanotoxicology* 11, 405–418. <https://doi.org/10.1080/17435390.2017.1309703>.
- Cornick, S., Tawiah, A., Chadee, K., 2015. Roles and regulation of the mucus barrier in the gut. *Tissue Barriers* 3, 982426. <https://doi.org/10.4161/21688370.2014.982426>.
- Cowger, W., Steinmetz, Z., Gray, A., Munno, K., Lynch, J., Hapich, H., Primpke, S., De Frond, H., Rochman, C., Herodotou, O., et al., 2021. Microplastic Spectral Classification Needs an Open Source Community: Open Specy to the Rescue! *Analytical Chem.* <https://doi.org/10.1021/acs.analchem.1c00123>.
- De Felice, B., Bacchetta, R., Santo, N., Tremolada, P., Parolini, M., 2018. Polystyrene microplastics did not affect body growth and swimming activity in *Xenopus laevis* tadpoles. *Environ. Sci. Pollut. Res.* 25, 34644–34651. <https://doi.org/10.1007/s11356-018-3408-x>.
- Duan, Z., Duan, X., Zhao, S., Wang, X., Wang, J., Liu, Y., Peng, Y., Gong, Z., Wang, L., 2020. Barrier function of zebrafish embryonic chorions against microplastics and nanoplastics and its impact on embryo development. *J. Hazard. Mater.* 395, 122621. <https://doi.org/10.1016/j.jhazmat.2020.122621>.
- EFSA, 2016. Presence of microplastics and nanoplastics in food, with particular focus on seafood. *EFSA J.* 14, 4501. <https://doi.org/10.2903/j.efsa.2016.4501>.
- Eitzen, L., Paul, S., Braun, U., Altmann, K., Jekel, M., Ruhl, A.S., 2019. The challenge in preparing particle suspensions for aquatic microplastic research. *Environ. Res.* 168, 490–495. <https://doi.org/10.1016/j.envres.2018.09.008>.
- El Hadri, H., Gigault, J., Maxit, B., Grassl, B., Reynaud, S., 2020. Nanoplastic from mechanically degraded primary and secondary microplastics for environmental assessments. *NanoImpact* 17, 100206. <https://doi.org/10.1016/j.impact.2019.100206>.
- Eriksen, M., Lebreton, L.C.M., Carson, H.S., Thiel, M., Moore, C.J., Borerro, J.C., Galgani, F., Ryan, P.G., Reisser, J., 2014. Plastic pollution in the world's oceans: more than 5 trillion plastic pieces weighing over 250,000 tons afloat at sea. *PLoS One* 9, 111913. <https://doi.org/10.1371/journal.pone.0111913>.
- Espinosa, C., Esteban, M.A., Cuesta, A., 2019. Dietary administration of PVC and PE microplastics produces histological damage, oxidative stress and immunoregulation in European sea bass (*Dicentrarchus labrax* L.). *Fish Shellfish Immunol.* 95, 574–583. <https://doi.org/10.1016/j.fsi.2019.07.022>.
- Felsing, S., Kochleus, C., Buchinger, S., Brennholt, N., Stock, F., Reifferscheid, G., 2018. A new approach in separating microplastics from environmental samples based on their electrostatic behavior. *Environ. Pollut.* 234, 20–28. <https://doi.org/10.1016/j.envpol.2017.11.013>.
- Fendall, L.S., Sewell, M.A., 2009. Contributing to marine pollution by washing your face: microplastics in facial cleansers. *Mar. Pollut. Bull.* 58, 1225–1228. <https://doi.org/10.1016/j.marpolbul.2009.04.025>.
- Fiandra, L., Bonfanti, P., Piuino, Y., Nagvenkar, A.P., Perlestein, I., Gedanken, A., Saibene, M., Colombo, A., Mantecca, P., 2020. Hazard assessment of polymer-capped CuO and ZnO nanocolloids: a contribution to the safe-by-design implementation of biocidal agents. *NanoImpact* 17, 100195. <https://doi.org/10.1016/j.impact.2019.100195>.
- Finney, D.J., 1971. *Probit Analysis*. Cambridge Univ. Press, London.
- Fu, W., Min, J., Jiang, W., Li, Y., Zhang, W., 2020. Separation, characterization and identification of microplastics and nanoplastics in the environment. *Sci. Total Environ.* 721, 137561. <https://doi.org/10.1016/j.scitotenv.2020.137561>.
- GESAMP Joint Group of Experts on the Scientific Aspects of Marine Environmental Protection, 2015. Sources, fate and effects of microplastics in the marine environment: a global assessment". *Reports Stud. GESAMP* 90, 96. <https://doi.org/10.13140/RG.2.1.3803.7925>.
- Geyer, R., Jambeck, J.R., Law, K.L., 2017. Production, use, and fate of all plastics ever made. *Sci. Adv.* 3, 1700782. <https://doi.org/10.1126/sciadv.1700782>.
- Giani, D., Baini, M., Galli, M., Casini, S., Fossi, M.C., 2019. Microplastics occurrence in edible fish species (*Mullus barbatus* and *Merluccius merluccius*) collected in three different geographical sub-areas of the Mediterranean Sea. *Mar. Pollut. Bull.* 140, 129–137. <https://doi.org/10.1016/j.marpolbul.2019.01.005>.
- Gigault, J., Pedrono, B., Maxit, B., Ter Halle, A., 2016. Marine plastic litter: the unanalyzed nano-fraction. *Environ. Sci. Nano* 3, 346–350. <https://doi.org/10.1039/c6en00008h>.
- Haque, E., Ward, A., 2018. Zebrafish as a model to evaluate nanoparticle toxicity. *Nanomaterials* 8, 561. <https://doi.org/10.3390/nano8070561>.
- Hawkins, K.R., Yager, P., 2003. Nonlinear decrease of background fluorescence in polymer thin-films - a survey of materials and how they can complicate fluorescence detection in  $\mu$ TAS. *Lab Chip* 3, 248–252. <https://doi.org/10.1039/b307772c>.
- Jabeen, K., Li, B., Chen, Q., Su, L., Wu, C., Hollert, H., Shi, H., 2018. Effects of virgin microplastics on goldfish (*Carassius auratus*). *Chemosphere* 213, 323–332. <https://doi.org/10.1016/j.chemosphere.2018.09.031>.
- Koongolla, J.B., Lin, L., Pan, Y.F., Yang, C.P., Sun, D.R., Liu, S., Xu, X.R., Maharana, D., Huang, J.S., Li, H.X., 2020. Occurrence of microplastics in gastrointestinal tracts and gills of fish from Beibu Gulf, South China Sea. *Environ. Pollut.* 258, 113734. <https://doi.org/10.1016/j.envpol.2019.113734>.
- Law, K.L., 2017. Plastics in the Marine Environment. *Ann. Rev. Mar. Sci.* 9, 205–229. <https://doi.org/10.1146/annurev-marine-010816-060409>.
- Lee, H., Shim, W.J., Kwon, J.H., 2014. Sorption capacity of plastic debris for hydrophobic organic chemicals. *Sci. Total Environ.* 470–471, 1545–1552. <https://doi.org/10.1016/j.scitotenv.2013.08.023>.
- Lei, L., Wu, S., Lu, S., Liu, M., Song, Y., Fu, Z., Shi, H., Raley-Susman, K.M., He, D., 2018. Microplastic particles cause intestinal damage and other adverse effects in zebrafish *Danio rerio* and nematode *Caenorhabditis elegans*. *Sci. Total Environ.* 619–620, 1–8. <https://doi.org/10.1016/j.scitotenv.2017.11.103>.
- Lema, S.C., Schultz, I.R., Scholz, N.L., Incardona, J.P., Swanson, P., 2007. Neural defects and cardiac arrhythmia in fish larvae following embryonic exposure to 2,2',4,4'-tetrabromodiphenyl ether (PBDE 47). *Aquat. Toxicol.* 82, 296–307. <https://doi.org/10.1016/j.aquatox.2007.03.002>.
- Li, C., Busquets, R., Campos, L.C., 2020. Assessment of microplastics in freshwater systems: a review. *Sci. Total Environ.* <https://doi.org/10.1016/j.scitotenv.2019.135578>.
- Lu, Y., Zhang, Y., Deng, Y., Jiang, W., Zhao, Y., Geng, J., Ding, L., Ren, H., 2016. Uptake and accumulation of polystyrene microplastics in zebrafish (*Danio rerio*) and toxic effects in liver. *Environ. Sci. Technol.* 50, 4054–4060. <https://doi.org/10.1021/acs.est.6b00183>.
- Lusher, A., 2015. Microplastics in the marine environment: distribution, interactions and effects. In: *Marine Anthropogenic Litter*. Springer International Publishing, pp. 245–307. [https://doi.org/10.1007/978-3-319-16510-3\\_10](https://doi.org/10.1007/978-3-319-16510-3_10).
- Manabe, M., Tatarazako, N., Kinoshita, M., 2011. Uptake, excretion and toxicity of nano-sized latex particles on medaka (*Oryzias latipes*) embryos and larvae. *Aquat. Toxicol.* 105, 576–581. <https://doi.org/10.1016/j.aquatox.2011.08.020>.

- Mantecca, P., Moschini, E., Bonfanti, P., Fascio, U., Perelshtein, I., Lipovsky, A., Chirico, G., Bacchetta, R., Del Giacco, L., Colombo, A., Gedanken, A., 2015. Toxicity evaluation of a new Zn-doped CuO nanocomposite with highly effective antibacterial properties. *Toxicol. Sci.* 146, 16–30. <https://doi.org/10.1093/toxsci/kfv067>.
- Markic, A., Gaertner, J.C., Gaertner-Mazouni, N., Koelmans, A.A., 2019. Plastic ingestion by marine fish in the wild. *Crit. Rev. Environ. Sci. Technol.* 50, 657–697. <https://doi.org/10.1080/10643389.2019.1631990>.
- Mazurais, D., Ernande, B., Quazuguel, P., Severe, A., Huelvan, C., Madec, L., Mouchel, O., Soudant, P., Robbins, J., Huvet, A., Zambonino-Infante, J., 2015. Evaluation of the impact of polyethylene microbeads ingestion in European sea bass (*Dicentrarchus labrax*) larvae. *Mar. Environ. Res.* 112, 78–85. <https://doi.org/10.1016/j.marenvres.2015.09.009>.
- Messinetti, S., Mercurio, S., Parolini, M., Sugni, M., Pennati, R., 2018. Effects of polystyrene microplastics on early stages of two marine invertebrates with different feeding strategies. *Environ. Pollut.* 237, 1080–1087. <https://doi.org/10.1016/j.envpol.2017.11.030>.
- Naidoo, T., Glassom, D., 2019. Decreased growth and survival in small juvenile fish, after chronic exposure to environmentally relevant concentrations of microplastic. *Mar. Pollut. Bull.* 145, 254–259. <https://doi.org/10.1016/j.marpolbul.2019.02.037>.
- Neves, D., Sobral, P., Ferreira, J.L., Pereira, T., 2015. Ingestion of microplastics by commercial fish off the Portuguese coast. *Mar. Pollut. Bull.* 101, 119–126. <https://doi.org/10.1016/j.marpolbul.2015.11.008>.
- Ng, A.N.Y., De Jong-Curtain, T.A., Mawdsley, D.J., White, S.J., Shin, J., Appel, B., Dong, P.D.S., Stainier, D.Y.R., Heath, J.K., 2005. Formation of the digestive system in zebrafish: III. Intestinal epithelium morphogenesis. *Dev. Biol.* 286, 114–135. <https://doi.org/10.1016/j.ydbio.2005.07.013>.
- Nieuwkoop, P., Faber, J., 1956. Nieuwkoop PD, Faber J (1956) Normal table of *Xenopus laevis* (DAUDIN). A systematic and chronological survey of the development from the fertilized egg till the end. Amsterdam: North Holland Publishing Co. 260 p. - Open Access Library [WWW Document]. <https://www.oalib.com/references/10915515> (Accessed 21 July 2020).
- Nobre, C.R., Santana, M.F.M., Maluf, A., Cortez, F.S., Cesar, A., Pereira, C.D.S., Turra, A., 2015. Assessment of microplastic toxicity to embryonic development of the sea urchin *Lytechinus variegatus* (Echinodermata: Echinoidea). *Mar. Pollut. Bull.* 92, 99–104. <https://doi.org/10.1016/j.marpolbul.2014.12.050>.
- O'Donovan, S., Mestre, N.C., Abel, S., Fonseca, T.G., Carteny, C.C., Cormier, B., Keiter, S.H., Bebianno, M.J., 2018. Ecotoxicological effects of chemical contaminants adsorbed to microplastics in the Clam *Scrobicularia plana*. *Front. Mar. Sci.* 5, 143. <https://doi.org/10.3389/fmars.2018.00143>.
- OECD, 2013. Test No. 236: Fish Embryo Acute Toxicity (FET) Test. OECD Guidel. Test. Chem. Sect. 2, OECD Publ. 1–22. <https://doi.org/10.1787/9789264203709-en>.
- Ong, K.J., Zhao, X., Thistle, M.E., McCormack, T.J., Clark, R.J., Ma, G., Martinez-Rubi, Y., Simard, B., Loo, J.S.C., Veinot, J.G.C., Goss, G.G., 2014. Mechanistic insights into the effect of nanoparticles on zebrafish hatch. *Nanotoxicology* 8, 295–304. <https://doi.org/10.3109/17435390.2013.778345>.
- Pannetier, P., Morin, B., Le Bihanic, F., Dubreil, L., Clérandeau, C., Chouvellon, F., Van Arkel, K., Danion, M., Cachot, J., 2020. Environmental samples of microplastics induce significant toxic effects in fish larvae. *Environ. Int.* 134, 105047. <https://doi.org/10.1016/j.envint.2019.105047>.
- Pedà, C., Caccamo, L., Fossi, M.C., Gai, F., Andaloro, F., Genovese, L., Perdichizzi, A., Romeo, T., Maricchiolo, G., 2016. Intestinal alterations in European sea bass *Dicentrarchus labrax* (Linnaeus, 1758) exposed to microplastics: preliminary results. *Environ. Pollut.* 212, 251–256. <https://doi.org/10.1016/j.envpol.2016.01.083>.
- Phuong, N.N., Zalouk-Vergnoux, A., Poirier, L., Kamari, A., Châtel, A., Mouneyrac, C., Lagarde, F., 2016. Is there any consistency between the microplastics found in the field and those used in laboratory experiments? *Environ. Pollut.* 211, 111–123. <https://doi.org/10.1016/j.envpol.2015.12.035>.
- Pitt, J.A., Kozal, J.S., Jayasundara, N., Massarsky, A., Trevisan, R., Geitner, N., Wiesner, M., Levin, E.D., Di Giulio, R.T., 2018. Uptake, tissue distribution, and toxicity of polystyrene nanoparticles in developing zebrafish (*Danio rerio*). *Aquat. Toxicol.* 194, 185–194. <https://doi.org/10.1016/j.aquatox.2017.11.017>.
- Qiu, Q., Peng, J., Yu, X., Chen, F., Wang, J., Dong, F., 2015. Occurrence of microplastics in the coastal marine environment: first observation on sediment of China. *Mar. Pollut. Bull.* 98, 274–280. <https://doi.org/10.1016/j.marpolbul.2015.07.028>.
- Rainieri, S., Conlledo, N., Larsen, B.K., Granby, K., Barranco, A., 2018. Combined effects of microplastics and chemical contaminants on the organ toxicity of zebrafish (*Danio rerio*). *Environ. Res.* 162, 135–143. <https://doi.org/10.1016/j.envres.2017.12.019>.
- Rist, S., Hartmann, N.B., 2018. Aquatic ecotoxicity of microplastics and nanoplastics: lessons learned from engineered nanomaterials. In: *Handbook of Environmental Chemistry*. Springer Verlag, pp. 25–49. [https://doi.org/10.1007/978-3-319-61615-5\\_2](https://doi.org/10.1007/978-3-319-61615-5_2).
- Rist, S., Baun, A., Hartmann, N.B., 2017. Ingestion of micro- and nanoplastics in *Daphnia magna* – quantification of body burdens and assessment of feeding rates and reproduction. *Environ. Pollut.* 228, 398–407. <https://doi.org/10.1016/j.envpol.2017.05.048>.
- de Sá, L.C., Oliveira, M., Ribeiro, F., Rocha, T.L., Futter, M.N., 2018. Studies of the effects of microplastics on aquatic organisms: what do we know and where should we focus our efforts in the future? *Sci. Total Environ.* 645, 1029–1039. <https://doi.org/10.1016/j.scitotenv.2018.07.207>.
- Savoca, S., Bottari, T., Fazio, E., Bonsignore, M., Mancuso, M., Luna, G.M., Romeo, T., D'Urso, L., Capillo, G., Panarello, G., Greco, S., Compagnini, G., Lanteri, G., Crupi, R., Neri, F., Spanò, N., 2020. Plastics occurrence in juveniles of *Engraulis encrasicolus* and *Sardina pilchardus* in the Southern Tyrrhenian Sea. *Sci. Total Environ.* 718, 137457. <https://doi.org/10.1016/j.scitotenv.2020.137457>.
- Setälä, O., Fleming-Lehtinen, V., Lehtiniemi, M., 2014. Ingestion and transfer of microplastics in the planktonic food web. *Environ. Pollut.* 185, 77–83. <https://doi.org/10.1016/j.envpol.2013.10.013>.
- Sfriso, A.A., Tomio, Y., Rosso, B., Gambaro, A., Sfriso, A., Corami, F., Rastelli, E., Corinaldesi, C., Mistri, M., Munari, C., 2020. Microplastic accumulation in benthic invertebrates in Terra Nova Bay (Ross Sea, Antarctica). *Environ. Int.* 137, 105587. <https://doi.org/10.1016/j.envint.2020.105587>.
- Simon, S., Röhrs, S., 2018. Between fakes, forgeries, and illicit artifacts—authenticity studies in a heritage science laboratory. *Arts* 7, 20. <https://doi.org/10.3390/arts702020>.
- Song, Y.K., Hong, S.H., Jang, M., Han, G.M., Jung, S.W., Shim, W.J., 2017. Combined effects of UV exposure duration and mechanical abrasion on microplastic fragmentation by polymer type. *Environ. Sci. Technol.* 51, 4368–4376. <https://doi.org/10.1021/acs.est.6b06155>.
- Sotres, J., Jankovskaja, S., Wannerberger, K., Arnebrant, T., 2017. Ex-vivo force spectroscopy of intestinal mucosa reveals the mechanical properties of mucus blankets. *Sci. Rep.* 7, 1–14. <https://doi.org/10.1038/s41598-017-07552-7>.
- Ter Halle, A., Jeanneau, L., Martignac, M., Jardé, E., Pedrono, B., Brach, L., Gigault, J., 2017. Nanoplastic in the North Atlantic subtropical gyre. *Environ. Sci. Technol.* 51, 13689–13697. <https://doi.org/10.1021/acs.est.7b03667>.
- van Pomeran, M., Brun, N.R., Peijnenburg, W.J.G.M., Vijver, M.G., 2017. Exploring uptake and biodistribution of polystyrene (nano)particles in zebrafish embryos at different developmental stages. *Aquat. Toxicol.* 190, 40–45. <https://doi.org/10.1016/j.aquatox.2017.06.017>.
- Wang, F., Wong, C.S., Chen, D., Lu, X., Wang, F., Zeng, E.Y., 2018. Interaction of toxic chemicals with microplastics: a critical review. *Water Res.* <https://doi.org/10.1016/j.watres.2018.04.003>.
- Wang, Z.M., Wagner, J., Ghosal, S., Bedi, G., Wall, S., 2017. SEM/EDS and optical microscopy analyses of microplastics in ocean trawl and fish guts. *Sci. Total Environ.* 603–604, 616–626. <https://doi.org/10.1016/j.scitotenv.2017.06.047>.
- Yang, H., Xiong, H., Mi, K., Xue, W., Wei, W., Zhang, Y., 2020. Toxicity comparison of nano-sized and micron-sized microplastics to Goldfish *Carassius auratus* Larvae. *J. Hazard. Mater.* 388, 122058. <https://doi.org/10.1016/j.jhazmat.2020.122058>.
- Zhang, R., Silic, M.R., Schaber, A., Wasel, O., Freeman, J.L., Sepúlveda, M.S., 2020. Exposure route affects the distribution and toxicity of polystyrene nanoplastics in zebrafish. *Sci. Total Environ.* 724, 138065. <https://doi.org/10.1016/J.SCITOTENV.2020.138065>.